Estuaries and Coasts (2024) 47:567–587
https://doi.org/10.1007/s12237-023-01277-9

Marine and Not Terrestrial Resources Support Nearshore Food Webs Across a Gradient of Glacial Watersheds in the Northern Gulf of Alaska

James Schloemer[1,2] · Lee Ann Munk[3] · Katrin Iken[2]

Received: 6 March 2023 / Revised: 31 August 2023 / Accepted: 4 September 2023 / Published online: 3 October 2023
© The Author(s) 2023

Abstract

Estuaries are among the most productive ecosystems on Earth, yet they are at risk in high-latitude regions due to climate-driven effects on the connected terrestrial and marine realms. Northern Hemisphere warming exceeds the global average and accelerates the melting of glaciers. As a result, the magnitude of freshwater discharge into estuaries may increase during the peak in glacial meltwater, ultimately affecting the riverine flux of organic matter (OM) from the land to coastal environments and food webs within. We investigated the extent to which terrestrial OM subsidizes nearshore food webs in northern Gulf of Alaska watersheds and if differences in the relative proportion of terrestrial versus marine OM supporting these food webs are explained by watershed glacial cover and/or by seasonal glacial discharge regimes. A stable isotope mixing model was employed to determine the contribution of marine (phytoplankton, macroalgae) and terrestrial (vascular plant) sources to the diets of grazing/detritivore and filter/suspension-feeding coastal invertebrates at the outflows of watersheds of varying glacial influence and across three distinct discharge periods. Additionally, a distance-based redundancy analysis was conducted to investigate the effects of watershed-characteristic (e.g., slope, vegetation cover) sourcing and transport of terrestrial OM on consumer diets. The diets of both feeding groups were predominantly marine (> 90%) and varied little among estuarine study sites at watersheds of different glacial cover or glacial discharge periods. Our findings suggest that terrestrial OM is not readily used by nearshore food webs in this productive study system, presumably due to the high quantity and quality of available marine OM.

Keywords Nearshore food webs · Glacier runoff · Stable isotopes · Marine ecosystems

Introduction

River systems are responsible for transporting large quantities of terrestrially derived organic matter (OM) to the world's oceans, delivering an estimated 0.43 Gt of organic carbon each year worldwide (Hope et al. 1994; Schlünz and Schneider 2000; Li et al. 2019). Such allochthonous subsidies delivered to coastal systems can either augment marine food webs with additional food sources or compromise them with lower nutritional content; though, the value of these subsidies may vary based on a unique system's need for specific sources of nutrition at a given time. For instance, mangrove-derived detritus is an essential component in decapod crustacean and fish diets (Claudino et al. 2015). Yet, it is most used at upper estuarine locations where mangrove detritus is more available than marine primary production (Ray et al. 2018). Thus, the proximity of consumers to an OM source can be key in controlling which resources are being used. In estuaries, upstream and coastal habitats are connected through the movement of water, which can transport OM among locations. While marine-sourced OM can be the sole food source in some estuarine food webs (Guest and Connolly 2005; Ray et al. 2018), in other systems river flow advects allochthonous OM from terrestrial sources to adjoining coastal areas to support marine food webs (Howe and Simenstad 2015). Diverse resource use is particularly relevant to ecosystems experiencing high variability among

Communicated by Kenneth Dunton

✉ James Schloemer
jwschloemer@alaska.edu

[1] Kachemak Bay National Estuarine Research Reserve, Homer, AK, USA

[2] College of Fisheries and Ocean Sciences, University of Alaska Fairbanks, Fairbanks, AK, USA

[3] Department of Geological Sciences, University of Alaska Anchorage, Anchorage, AK, USA

seasons, such as some Arctic systems, where OM_{terr} constituted up to 40% of the diets of marine taxa spanning four trophic guilds (Harris et al. 2018). Similarly, nearshore consumers in a high-latitude estuarine system in Alaska were able to connect slower-producing (macroalgal-based, terrestrial) and faster-producing (phytoplankton-based) trophic pathways, depending on local environmental conditions (Siegert et al. 2022). These research efforts exemplify the growing recognition of the utility of terrestrial subsidies to coastal ecosystems but highlight the need to understand how these resources are portioned among feeding groups in different ecosystems.

Estuarine productivity is traditionally associated with the convergence of upland resources, in situ estuarine production, and OM from marine sources (Canuel and Hardison 2016). In high-latitude regions, estuarine systems experience added complexity from the influx of glacial meltwater where cold, turbid water from glaciers can modify downstream conditions in local estuaries. The relative proportion of glacial input to a watercourse will ultimately affect estuarine temperature, light attenuation (Ren et al. 2019), nutrient concentrations (Hood and Scott 2008; Jenckes et al. 2022), and discharge volume (Sergeant et al. 2020). The influence of glaciers on OM_{terr} delivery was recognized in southeast Alaskan estuarine food webs, where select invertebrates (e.g., *Mytilus trossulus*) displayed greater assimilation of OM_{terr} at locations of greater glacial influence (Arimitsu et al. 2018). Glaciers store and release considerable amounts of OM_{terr} in dissolved and particulate forms (Ren et al. 2019), of which dissolved material is highly labile due to modification over long periods spent trapped in ice (Hood et al. 2009). Particulate OM can be less labile due to larger surface area-to-mass ratios and association with mineral particles, but the bioavailability can increase after undergoing physical and chemical breakdown during transit through river systems. Vascular land plants also contribute to particulate OM delivered to the estuary but contain high quantities of recalcitrant fiber in their cell walls, which requires microbial processing before becoming usable by marine consumers (Arnosti 2011).

To an individual marine consumer, OM from vascular plants is of lower nutritional quality because the quantity of recalcitrant fiber is proportionally greater than other nutrients (carbohydrates, proteins, lipids) and, thus, yields less energy per unit of organic matter consumed (Varga and Kolver 1997). On a system-wide scale, the extra microbial processing step between terrestrial primary production and marine consumers is associated with decreased energy transfer efficiency due to a lengthened food web (Berglund et al. 2007). Conversely, the increased bioavailability of glacially derived OM, when compared to fresh plant material, makes older glacial carbon a key resource in proglacial stream food webs (Fellman et al. 2015) and could be assumed to also contribute to the downstream, estuarine systems. If OM_{terr} serves as an allochthonous subsidy to nearshore consumers, the efficiency of coastal food webs may be susceptible to changes in OM_{terr} supply. For example, if the ratio of labile glacial OM to refractory upland OM_{terr} changes with discharge volume, the utilization of refractory OM_{terr} by consumers in downstream estuarine environments may change accordingly.

Climate change is projected to cause a global decrease in glacial volume by 25–48% between 2010 and 2100 (Huss and Hock 2018). This will lead to an increase in the flux of OM from terrestrial and glacial sources to high-latitude coastal ecosystems (Fellman et al. 2010; Hood et al. 2015; Lafrèniere and Sharp, 2005; O'Neel et al. 2015). Furthermore, the frequent flushing of watersheds associated with extreme weather is expected to contribute to these dissolved and particulate OM loads (Wheatcroft et al. 2010; Hounshell et al. 2019). Glacial ice covers nearly 10% of the land area on Earth's surface and stores roughly 6 Gt of organic carbon (OC) (Hood et al. 2015). Due to their dynamic nature, glacial landscapes are often characterized by steep-gradient watersheds with relatively short river reaches. In these landscapes, the relative proportion of particulate OC (POC) sources (e.g., lithology, soils, plant litter) derived from glacial discharge may change with climate warming due to decreased physical weathering associated with glacier retreat and the subsequent establishment of primary-successive vegetation. Furthermore, in mountain ecosystems, tundra is diminishing as shrub and tree lines advance at a rate closely matching climate velocity (Dial et al. 2016). This increase in plant- and soil-derived POC, decrease in geogenic POC, and compositional change of plant-derived POC from tundra to a shrub-tree community will ultimately change the chemical and nutritional composition of stream organic aggregates as they are transported to the estuarine environment. This increased flux of OC driven by environmental change is likely to influence downstream ecosystem processes and food webs in associated estuaries.

Glaciers and ice fields supply 47% of freshwater runoff to the Gulf of Alaska (GoA; Neal et al. 2010) and help regulate coastal productivity through the supply of critical nutrients and OM (Hood et al. 2009; Tranter and Wadham 2013; Arimitsu et al. 2018). The quantity of freshwater sourced from glacial melt in the GoA is tightly linked to air temperature (Radić et al. 2014) and is susceptible to change in this region, where the rate of warming exceeds global mean trends (IPCC 2007). A recent study by Huss and Hock (2018) found that nearly 50% of the large-scale glacial basins (> 5000 km^2) on Earth have already reached peak meltwater, and that the remaining basins are estimated to peak by the end of the twenty-first century; three of these remaining basins drain into the GoA (Alsek, Copper, Susitna rivers). Considering these estimates, the proportion of

terrestrial resources delivered to the GoA region will likely continue to increase until glaciers approach peak meltwater and later decrease following the decline of peak meltwater with decreasing glacial mass (Hood and Scott 2008). Despite long-term change, short-term variability is expected as interannual patterns in freshwater discharge are subject to local climate conditions. On the seasonal scale, freshwater discharge in the GoA region is generally expected to peak mid-summer, owing to increased solar radiation typical of high-latitude areas (Sergeant et al. 2020).

Marine invertebrate communities are a key trophic pathway in the transfer of producer-fixed carbon to higher trophic levels, serving as prey for fish, seabirds, and marine mammals, and resources for subsistence and commercial harvests by humans. In the GoA region, marine invertebrates not only are a subsistence resource but also are of cultural significance and commonly incorporated into art and lore. These invertebrates vary based on taxonomic and functional groups, which depend, in part, on the habitat in which an organism lives and the resources available. For example, suspension-feeding organisms can be limited to ingesting particles of a particular size within the water column and may be nonselective based on food quality (Ward and Shumway 2004) whereas deposit-feeding or grazing organisms may mobilize to access desired food items when they are not immediately accessible (Ward and Shumway 2004; Kamio and Derby, 2017). As a result, the feeding strategy of a consumer may dictate the amount of OM ingested from marine and terrestrial origins, but access to OM will also be strongly modulated by climatic conditions and the availability of suitable resources to select feeding groups when needed (Cauvy-Fraunié and Dangles 2019).

This study evaluated the contribution of OM_{terr} to estuarine systems and the diets of select high-latitude coastal invertebrate consumers along a gradient of glacial coverage of watersheds in the northern GoA. Here, a series of watersheds with increasing glacial coverage (0–60%) set the framework of a gradient in the magnitude of effect glacial discharge points may have on coastal food webs. Seasonal flow periods elucidate how patterns in freshwater discharge are indicative of OM_{terr} sourcing and transport to the nearshore. Thus, this system may serve as a model to illustrate how coastal food webs are affected by varying OM_{terr} delivery from glacial melt at high latitudes. As such, the goal of this study was to quantify and understand the effects of glacial influence on resource use by common high-latitude coastal invertebrates, which serve as a key food resource at higher tropic levels and are culturally important to subsistence communities. The goal was addressed with three hypotheses: (1) terrestrial resources will contribute more to invertebrate diets in watersheds of higher glaciation and during higher discharge periods, (2) filter-feeding invertebrates will use more OM_{terr} than grazers across all watersheds, and (3) watershed drivers associated with glaciation (e.g., slope, vegetation cover) will influence consumer diets.

Materials and Methods

Study Sites and Design

The study was carried out in Kachemak Bay, Alaska, which is an example of a fjord-type, glacially influenced estuary contiguous to Cook Inlet in the central GoA (Fig. 1). The bay is characterized on the southern side by steep mountains and high-gradient watersheds with a mix of deep side-fjords and shallow bays. Freshwater input is sourced from the meltwater of glaciers and snowpack in addition to small streams and precipitation. Large tides, sometimes exceeding 8 m, contribute to the transport and mixing of marine and terrestrial organic materials within the bay (Muench et al. 1978).

The study was conducted from May 2019 through September 2020 at five estuarine sites located in separate watersheds along the southern shore of Kachemak Bay: Jakolof Bay (JAK), Tutka Bay (TUT), Wosnesenski River (WOS), Halibut Cove (HAL), and Grewingk Glacier (GRW) (Fig. 1). These locations were selected because the watersheds represent a gradient of glacier coverage, calculated as the percent of glacier coverage of the respective watershed area. Across sites, watershed composition ranged from 0% glaciated and 65% forested (JAK) to 60% glaciated and 4% forested (GRW), with a river-flow minimum reach of 3.9 km (JAK) and a maximum of 25.8 km (WOS) (Table 1). The geology of the watersheds is characterized almost entirely by the McHugh complex (Kusky and Bradley 1999), which largely includes greywacke and conglomerate lithologies. Soils here are relatively thin and young and have not weathered intensely (Jenckes et al. 2023; Wiles and Calkin 1994). Sites varied in coastal form, with JAK, TUT, and HAL located near the head of side embayments, and WOS and GRW located directly in Kachemak Bay. While ideally, sites would be similar to control localized sources of variability, the discharge points (river mouths) from the watersheds dictated sampling locations. As a result, all sites were positioned approximately 1–1.5 km from the river mouths at high tide. During low tide, some side-embayed sites (JAK, TUT) were positioned immediately adjacent to the tidal river channel, while more open-bay sites with larger deltas (WOS, GRW) were still positioned 1–1.5 km from the active tidal river channel; at one side-embayment, the HAL site was consistently 1.5 km from the river mouth. There may exist site-specific processes affecting observations; for example, embayed sites may not flush as readily as non-embayed sites although the considerable tides in this region are likely to offset, at least in part, water

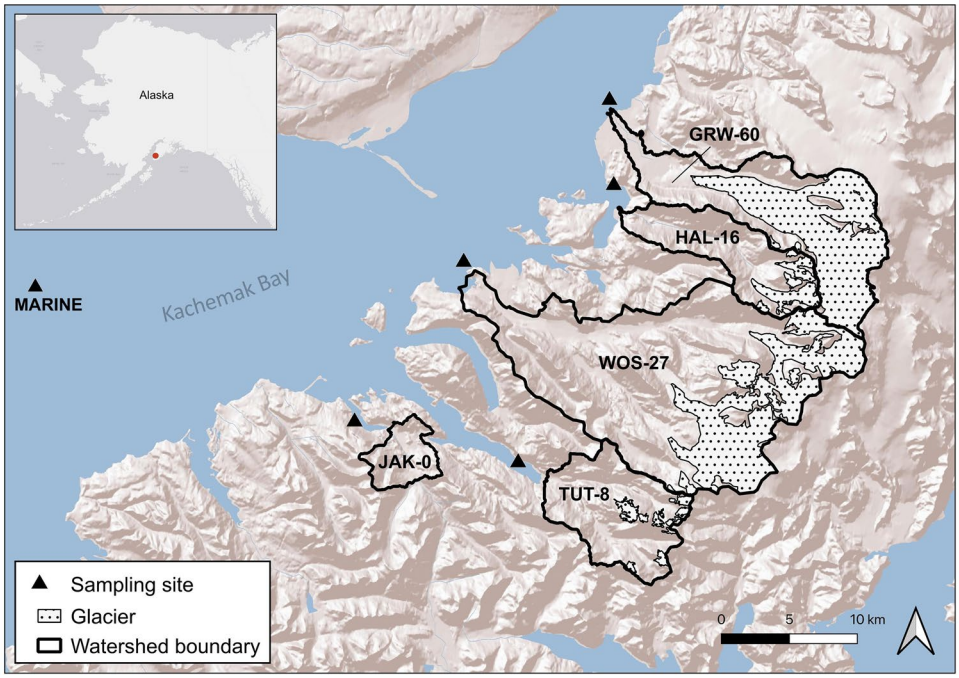

Fig. 1 Study site locations in Kachemak Bay, Alaska. Study sites are black triangles. Watershed boundaries are outlined in black. Glacial coverage is denoted with stippling. Glacial coverage was determined using 2012 SPOT 5 imagery and later validated using 2018 Sentinel imagery. Watersheds not reaching the estuarine cost (e.g., Jakolof, Tutka) is an artifact of the basemap design; coastlines may be defined by different tidal stages than the watershed boundary lower limits computed in this study

retention associated with bay length. Lower estuary morphology ranged from rocky and restricted (JAK, HAL, TUT) to wide floodplains (WOS, GRW). Peak freshwater discharge in the region occurs in mid-July in these glacial watersheds (Sergeant et al. 2020) owing to typically warm air temperatures and high solar radiation during that time of year. Across sites, mean seasonal salinities ranged between 18.8 and 28.8 psu (Supplement I, Table S6).

Primary Consumer and Diet-Source Collection

Samples were collected at each of the five sites three times per year, during characteristic river discharge stages in the GoA region: base flow (May–June), peak flow (July-August), and post-peak flow (September) in 2019 and 2020 (Sergeant et al. 2020). Sessile or low-mobility marine invertebrates were targeted as the primary consumers in these systems

Table 1 Watershed characteristics of the five study sites in Kachemak Bay, Alaska used in analysis of consumer stable isotope composition

	JAK	TUT	HAL	WOS	GRW
Static characteristics					
Area (km^2)	18.9	65.7	55.6	256.6	111.5
Glacial coverage (%)	0.0	8.0	16.1	27.0	60.0
Slope (S; %)	21.0	45.0	26.0	20.0	14.0
Mean elevation (E; m)	1140.0	1275.0	1494.0	1569.0	1641.0
Ruggedness (S/E)	0.02	0.04	0.02	0.01	0.01
Vegetation (%)	64.7	18.5	7.1	17.6	3.7
River length (km)	3.9	23.3	14.8	25.8	6.3
Dynamic characteristics*					
Discharge (m^3/s)	0.1 ± 0.2	6.6 ± 4.9	6.3 ± 2.9	31.9 ± 16.3	37.8 ± 13.8
TSS (mg/L)	2.1 ± 2.3	2.1 ± 3.9	22.4 ± 13.2	60.9 ± 32.4	56.6 ± 25.8

Static characteristics (unchanging during the study) were calculated using spatial statistics functions in ArcGIS 10.3 (see "Watershed Characteristics"). Dynamic characteristics (change throughout the study) are mean annual values during the study years and were made available by a partner project from river chemistry samples (Lee Ann Munk, University of Alaska Anchorage)

*Dynamic water chemistry data not used in analysis (DOC, DIC, TDN, DIN) are included in Supplement I, Table S1

and included grazers or detritivores (henceforth referred to as Gr/De; *Lottia* spp., *Littorina* spp.) and filter or suspension feeders (henceforth referred to as Su/FF; *Mytilus trossulus*, *Balanus* spp.). These taxa were selected due to their consistent presence across all locations, though other species and feeding modes were intermittently present at some of the sites. It is acknowledged that much of OM_{terr} enters the coastal system in detrital forms, thus biasing these feeding groups towards marine food sources. Still, limpets graze on biofilms and consume detrital particles within them, which expands their utility in this study to represent multiple feeding groups. Similarly, suspended detrital OM_{terr} particles feasibly are a food source for Su/FF. Species that were included in these feeding groups differed very little isotopically ($\delta^{13}C \pm 1$–2‰) during initial analyses, justifying the decision to group them. Three replicate individuals of each taxon were collected by hand from the intertidal zone at each site and sampling period. Muscle tissue was removed from each organism and dried at 60 °C until constant weight. Potential endmembers in the system collected included phytoplankton, estuarine particulate organic matter (POM_{estu}), common macroalgae, and vascular plants. Estimates of phytoplankton were assumed from POM samples collected offshore, approximately 15 km away from the influence of nearshore and river-born detritus. In contrast, POM_{estu} was collected nearshore in mid-glacial-plume waters at each site. Thus, POM_{estu} is likely a mix of marine and terrestrial resources that vary in proportion based on location and seasonal availability. For each POM sample type, two replicate water samples were collected at 5-m depth using a 5-L *General Oceanics* Niskin bottle and filtered onto a 0.7 µm Whatman GF/F filter (500–2000 ml); filters were then dried at 60 °C for 24 h. To obtain sufficient mass for sulfur isotope analysis, phytoplankton and POM_{estu} samples were also collected by 10-m vertical tows of a 20-µm mesh plankton net and centrifuged in 50-ml Falcon tubes until forming a pellet. The supernatant was siphoned off, and samples were dried at 60 °C until constant weight. Common macrophytes (including *Acrosiphonia* spp., *Fucus distichus*, *Saccharina latissima*, *Ulva* spp.) per site were collected from the intertidal zone and dried at 60 °C until constant weight. Only macroalgal species occurring at three or more sites were used in the analysis to facilitate the comparable assessment of sources among sites. Vascular plants were collected from saltmarsh (*Plantago maritima*, *Pucinellia* spp., *Triglochin maritima*) and upland locations (*Alnus* spp., *Populus trichocarpa*), and tissue was collected from the apical blade of leafing plants or the base stem of select marsh plants before drying at 60 °C.

Stable Isotope Measurements

All samples were analyzed for stable carbon and nitrogen isotopes ($\delta^{13}C$, $\delta^{15}N$), and select samples also for sulfur stable isotope ratios ($\delta^{34}S$). No sulfur isotope values were determined for samples from TUT, so this site was excluded from some of the analyses. Prior to analysis, POM samples were fumed with concentrated HCl vapors for 24 h to remove carbonates. Consumer, macrophyte, and vascular plant tissues were powdered using a Wig-L-Bug® dental mill prior to weighing into tin capsules for analyses. Lipids are typically depleted in ^{13}C, causing potential bias in carbon stable isotope analyses (DeNiro and Epstein 1977). One rule of thumb is that biological samples with a C:N ratio greater than ~ 6 are lipid contaminated (Abrantes et al. 2012), and should be lipid normalized prior to comparison (Post et al. 2007). In the present study, consumer muscle tissue C:N ratios were at or below this C:N ratio cutoff (Table 2). Although the C:N ratios of primary producers exceeded this cutoff greatly (C:N ratio > 10), C:N is not a good predictor of lipid content in plants (Post et al. 2007). Lastly, analysis of lipid correction of rocky intertidal invertebrates in the study region confirmed low lipid levels in species, making lipid correction unnecessary (Post et al. 2007; Siegert et al. 2022).

Stable carbon and nitrogen analysis was performed using continuous-flow isotope ratio mass spectrometry (IRMS) at the Alaska Stable Isotope Facility (ASIF) at the University of Alaska Fairbanks. A Costech ESC 4010 elemental analyzer was interfaced via a Conflo IV with a Thermo Finnigan Delta Vplus IRMS. Stable sulfur isotope analysis was performed using continuous-flow IRMS at the Stable Isotope Core Laboratory (SICL) at Washington State University using a Costech Analytical ECS 4010 elemental analyzer connected via a gas dilution to a Thermo Finnigan Delta PlusXP mass spectrometer. Results were expressed in the delta (δ) notation, meaning the normalized ratio in parts per thousand (per mil, ‰) according to the following equation:

$$\delta(‰) = ([R_{sample}/R_{standard}] - 1) * 1000,$$

where R is $^{13}C/^{12}C$, $^{15}N/^{14}N$, or $^{34}S/^{32}S$. Standards were Vienna Pee Dee Belemnite (VPDB) for $\delta^{13}C$ values, N^2 for $\delta^{15}N$ values, and Vienna Canyon Diablo Triolite (VCDT) for $\delta^{34}S$ values. The molar ratio of carbon to nitrogen (C:N ratio) was also calculated from the outputs of the carbon and nitrogen stable isotope analysis.

Stable Isotope Mixing Models

The effects of site and glacial discharge period on consumer stable isotope ratios were assessed using one-way permutational multivariate analyses of variance (PERMANOVA) in R package "vegan" v2.5–6 (Oksanen et al. 2019). To meet test assumptions, multivariate normality and homogeneity of dispersion were first checked using Mardia and Levene's tests, respectively, which deemed transformations unnecessary.

Table 2 Mean ± SD $\delta^{13}C$, $\delta^{15}N$, and $\delta^{34}S$ (‰) and molar C:N values of grazer/detrivore (Gr/De) and suspension/filter feeder (Su/FF) invertebrate groups, phytoplankton, estuarine particulate organic matter (POM_{estu}), and macroalgal, marsh, and upland diet sources

	Base					Peak					Post-peak				
Site/type	$\delta^{13}C$ (‰)	$\delta^{15}N$ (‰)	$\delta^{34}S$ (‰)	C:N	*n*	$\delta^{13}C$ (‰)	$\delta^{15}N$ (‰)	$\delta^{34}S$ (‰)	C:N	*n*	$\delta^{13}C$ (‰)	$\delta^{15}N$ (‰)	$\delta^{34}S$ (‰)	C:N	*n*
JAK-0															
Gr/De	−15.7 ± 0.8	8.9 ± 0.6	21.6 ± 0.0	3.7 ± 0.2	10	−16.0 ± 0.6	8.7 ± 0.8	20.7 ± 0.3	4.0 ± 0.3	12	−16.7 ± 1.8	8.8 ± 0.4	19.7 ± 0.9	3.9 ± 0.2	14
Su/FF	−17.3 ± 0.3	8.9 ± 0.5	19.2 ± 0.8	3.8 ± 0.6	12	−17.2 ± 0.4	9.6 ± 0.6	19.7 ± 0.5	3.9 ± 0.4	12	−17.3 ± 0.5	9.2 ± 0.8	18.9 ± 0.9	3.9 ± 0.7	12
Phytoplankton	−21.7 ± 0.6	4.9 ± 1.1	22.2 ± 0.2	6.1 ± 0.6	5	−21.3 ± 0.4	6.4 ± 0.7	19.6 ± 2.7	5.7 ± 0.8	4	−19.7 ± 0.6	5.5 ± 0.3	22.1 ± 0.7	6.0 ± 0.5	4
POM_{estu}	−20.0 ± 0.3	6.4 ± 1.0	19.5 ± 1.4	5.7 ± 0.5	7	−20.5 ± 0.2	6.6 ± 0.5	15.4 ± 3.8	6.0 ± 0.5	6	−20.3 ± 1.1	6.4 ± 0.8	13.9 ± 1.1	5.9 ± 0.2	6
Macroalgae	−17.6 ± 2.0	7.7 ± 0.6	21.9 ± 0.7	19.2 ± 7.8	32	−18.6 ± 2.6	6.2 ± 1.0	20.6 ± 1.0	29.9 ± 12.7	33	−17.0 ± 2.5	7.9 ± 0.9	20.6 ± 0.9	21.9 ± 18.1	21
Marsh Plant	−24.3 ± 1.3	3.4 ± 1.3	20.5 ± 1.1	16.1 ± 6.2	12	−23.9 ± 1.4	4.1 ± 2.9	18.6 ± 0.8	26.6 ± 17.5	12	−25.2 ± 1.6	4.5 ± 2.5	17.7 ± 1.0	27.6 ± 11.8	21
Upland Plant	−27.8 ± 1.6	−0.8 ± 2.3	9.2 ± 7.0	14.8 ± 2.7	9	−28.9 ± 1.4	−0.8 ± 2.9	5.1 ± 0.4	19.7 ± 3.8	9	−29.3 ± 2.0	−1.8 ± 2.3	4.1 ± 1.2	26.5 ± 7.8	15
TUT-8															
Gr/De	−17.2 ± 1.5	8.1 ± 0.5		3.9 ± 0.2	9	−16.6 ± 1.2	7.8 ± 0.6		4.0 ± 0.4	12	−17.4 ± 1.5	7.7 ± 0.5		3.9 ± 0.3	11
Su/FF	−18.3 ± 0.5	9 ± 1.0		4.2 ± 0.8	12	−18.4 ± 0.7	9.1 ± 0.6		4.0 ± 0.8	12	−18.3 ± 0.8	9.0 ± 0.6		4.0 ± 0.7	12
Phytoplankton	−21.7 ± 0.6	4.9 ± 1.1	22.2 ± 0.2	6.1 ± 0.6	5	−21.3 ± 0.4	6.4 ± 0.7	19.6 ± 2.7	5.7 ± 0.8	4	−19.7 ± 0.6	5.5 ± 0.3	22.1 ± 0.7	6.0 ± 0.5	4
POM_{estu}	−22.3 ± 2.1	6.5 ± 0.3	22.3 ± 0.7	6.6 ± 2.3	7	−22.3 ± 0.6	6.9 ± 1.9	16.9 ± 4.2	5.9 ± 1.0	6	−22.0 ± 1.4	6.8 ± 1.5	16.6 ± 0.5	5.9 ± 0.4	6
Macroalgae	−18.6 ± 2.7	5.1 ± 1.1		17.5 ± 11.0	21	−19.9 ± 2.5	4.7 ± 0.7		23.5 ± 15.9	33	−18.0 ± 4.1	6.6 ± 2.0		22.8 ± 20.4	23
Marsh Plant	−26.6 ± 0.9	1.5 ± 1.9		15.4 ± 7.4	12	−26.1 ± 1.9	2.9 ± 0.6		22.4 ± 5.8	12	−27.2 ± 1.6	2.7 ± 1.3		21.7 ± 6.8	24
Upland Plant	−27.2 ± 0.5	−2.3 ± 0.1		18.9 ± 1.5	3	−28.5 ± 1.3	−1.7 ± 0		21.2 ± 3.1	3	−29.7 ± 1.1	−1.5 ± 0.3		19.2 ± 2.7	6
HAL-16															
Gr/De	−15.8 ± 1.6	8.0 ± 0.7	20.9 ± 0.1	3.8 ± 0.2	11	−17.1 ± 2.4	7.9 ± 0.6	22.2 ± 1.4	3.8 ± 0.2	12	−16 ± 1.9	7.4 ± 0.6	21.1 ± 0.8	4.0 ± 0.2	12
Su/FF	−18.5 ± 0.9	8.5 ± 0.4	18.7 ± 0.1	3.9 ± 0.8	14	−18.6 ± 0.6	8.1 ± 0.6	20.7 ± 0.1	3.7 ± 0.4	12	−18.5 ± 0.6	8.5 ± 0.5	20.5 ± 0.2	4.0 ± 0.7	13
Phytoplankton	−21.7 ± 0.6	4.9 ± 1.1	22.2 ± 0.2	6.1 ± 0.6	5	−21.3 ± 0.4	6.4 ± 0.7	19.6 ± 2.7	5.7 ± 0.8	4	−19.7 ± 0.6	5.5 ± 0.3	22.1 ± 0.7	6.0 ± 0.5	4
POM_{estu}	−21.2 ± 0.4	6.1 ± 0.3	22.7 ± 1.4	6.0 ± 1.1	7	−22.0 ± 1.2	5.9 ± 1.9	21.4 ± 0.1	6.3 ± 1.1	6	−21.8 ± 0.7	6.4 ± 0.5	8.6 ± 0.4	6.2 ± 0.7	6
Macroalgae	−19.2 ± 3.3	4.9 ± 1.0	18.7 ± 3.4	18.8 ± 7.2	36	−20.1 ± 3.4	4.8 ± 0.7	21.3 ± 0.4	22.4 ± 10.6	38	−17.8 ± 3.5	5.8 ± 1.5	21.7 ± 0.5	18.9 ± 14.0	33
Marsh Plant	−24.6 ± 1.2	4.4 ± 1.1	18.4 ± 0.4	12.7 ± 3.0	12	−24.4 ± 1.4	4.4 ± 2.0	20.4 ± 0.6	23.0 ± 18.4	12	−25.4 ± 1.4	3.4 ± 2.1	18.8 ± 0.8	24.1 ± 12.5	24
Upland Plant	−27.7 ± 1.7	−0.9 ± 5.2	14.5 ± 0.4	16.3 ± 7.1	6	−27 ± 2.0	−2.5 ± 1.0	−3.3 ± 3.5	24.6 ± 9.4	6	−28.8 ± 1.5	−2.4 ± 1.1	−4.0 ± 0.5	24.6 ± 7.1	12
WOS-27															
Gr/De	−17.6 ± 0.8	8.6 ± 0.7	20.0 ± 0.3	3.9 ± 0.2	11	−17.4 ± 0.8	7.9 ± 1.6	20.0 ± 1.1	3.9 ± 0.1	12	−18.0 ± 1.1	8.1 ± 0.9	21.3 ± 1.0	3.9 ± 0.2	12
Su/FF	−18.1 ± 0.5	8.4 ± 0.9	19.4 ± 0.7	3.9 ± 0.6	12	−18.1 ± 0.5	8.3 ± 0.6	19.5 ± 1	3.8 ± 0.6	12	−17.9 ± 0.4	8.0 ± 1.0	20.8 ± 0.8	3.7 ± 0.4	12
Phytoplankton	−21.7 ± 0.6	4.9 ± 1.1	22.2 ± 0.2	6.1 ± 0.6	5	−21.3 ± 0.4	6.4 ± 0.7	19.6 ± 2.7	5.7 ± 0.8	4	−19.7 ± 0.6	5.5 ± 0.3	22.1 ± 0.7	6.0 ± 0.5	4
POM_{estu}	−21.7 ± 2.1	6.0 ± 1.8	18.9 ± 0	6.1 ± 0.8	7	−22.7 ± 0.7	6.1 ± 1.0	15.2 ± 0	6.8 ± 0.9	6	−22.3 ± 2.0	5.8 ± 0.3	19.2 ± 0.3	6.5 ± 1.8	6
Macroalgae	−19.4 ± 2.6	6.8 ± 1.1	21.1 ± 1.3	13.5 ± 5.9	26	−18.9 ± 2.3	7.2 ± 1.8	20.9 ± 0.7	12.7 ± 7.8	33	−16.9 ± 1.8	7.2 ± 1.2	21.6 ± 1.3	15.9 ± 12.1	36
Marsh Plant	−27.5 ± 1.8	4.4 ± 3.4	5.8 ± 0.7	15.1 ± 8.1	15	−24.0 ± 1.5	3.1 ± 2.6	14.6 ± 1.4	19.0 ± 4.8	9	−25.5 ± 2.4	2.3 ± 2.1	19.5 ± 3.0	24.3 ± 9.2	24
Upland Plant	−27.5 ± 1.0	−1.1 ± 0.4	12.1 ± 0.2	17.7 ± 4.3	6	−29.0 ± 0.4	−0.4 ± 0.3	−3.0 ± 0.1	23.4 ± 1.5	3	−30.3 ± 0.7	−0.8 ± 0.4	−4.5 ± 0.5	21.7 ± 3.9	6

Table 2 (continued)

Site/type	Base					Peak						Post-peak					
	$\delta^{13}C$ (‰)	$\delta^{15}N$ (‰)	$\delta^{34}S$ (‰)	C:N	*n*	$\delta^{13}C$ (‰)	$\delta^{15}N$ (‰)	$\delta^{34}S$ (‰)	C:N	*n*	$\delta^{13}C$ (‰)	$\delta^{15}N$ (‰)	$\delta^{34}S$ (‰)	C:N	*n*
GRW-60															
Gr/De	−16.8 ± 0.4	8.4 ± 0.3	20.6 ± 0.1	4.4 ± 0.9	6	−17.1 ± 0.8	8.4 ± 0.5	19.9 ± 0.4	4.1 ± 1.1	12	−16.8 ± 0.6	8.5 ± 0.6	21.8 ± 1.9	3.9 ± 0.2	12
Su/FF	−18.6 ± 0.7	8.6 ± 0.6	19.8 ± 0.7	4.6 ± 1.4	12	−18.9 ± 0.7	8.4 ± 0.5	19.8 ± 0.5	4.6 ± 1.2	12	−18.8 ± 0.6	8.5 ± 0.8	21.2 ± 1.2	4.1 ± 0.5	12
Phytoplankton	−21.7 ± 0.6	4.9 ± 1.1	22.2 ± 0.2	6.1 ± 0.6	5	−21.3 ± 0.4	6.4 ± 0.7	19.6 ± 2.7	5.7 ± 0.8	4	−19.7 ± 0.6	5.5 ± 0.3	22.1 ± 0.7	6.0 ± 0.5	4
POM_{estu}	−20.8 ± 0.6	7.3 ± 1.0	19.1 ± 1.2	5.6 ± 0.6	7	−24.0 ± 2.7	4.5 ± 3.3	20.8 ± 2.8	7.4 ± 3.4	10	−22.4 ± 1.1	6.4 ± 0.8	17.9 ± 1.3	5.9 ± 0.7	6
Macroalgae	−19.9 ± 2.6	6.3 ± 1.3	20.8 ± 0.6	24.7 ± 12.9	27	−21.9 ± 4.2	7.0 ± 1.8	20.5 ± 0.7	34.4 ± 18.9	27	−21.0 ± 7.0	6.9 ± 1.6	20.3 ± 2.8	22.5 ± 17.9	32
Marsh Plant	−24.9 ± 2.2	3 ± 2.2	20.1 ± 0.3	17.2 ± 4.9	12	−25.6 ± 1.7	3.2 ± 2.5	18.6 ± 0	18.6 ± 0.4	18	−26.8 ± 2.7	1.6 ± 3.0	17.0 ± 2.2	34.7 ± 14.2	21
Upland Plant	−28.1 ± 2.2	−2.7 ± 2.4	14.4 ± 0.2	18.0 ± 3.4	12	−28.5 ± 1.7	−3.5 ± 1.6	2.1 ± 7.1	21.5 ± 5.9	15	−29.2 ± 1.8	−3.3 ± 1.7	−2.6 ± 2.5	26.4 ± 10.3	15

All values were used as site-specific mixing models separated by the Kachemak Bay sampling site and discharge period (base, peak, post-peak). *n*, number of samples analyzed in each category. Numbers after site names indicate the percent glacial cover of the respective watershed

When significant site and glacial discharge period effects were detected, pairwise comparisons were run using a multilevel function that tests the null hypothesis of no difference in multivariate location between all possible pairs of groups. Specifically, the function calculates Bonferroni-corrected pseudo *p*-values based on permutations of the data. Similarity matrices for PERMANOVA were constructed using the Bray–Curtis similarity coefficient.

The proportional contribution of dietary sources to consumers was estimated using a Bayesian mixing model in the R package "MixSIAR" v3.1.12 (Stock et al. 2018). MixSIAR accounts for the uncertainty of isotope values from endmembers and consumers, trophic enrichment factors (TEF), and multiplicative error structures, accepts prior information, and can incorporate both categorical and continuous covariates (Stock et al. 2018). In this study, a four-tracer ($\delta^{13}C$, $\delta^{15}N$, $\delta^{34}S$, C:N) MixSIAR mixing model was used to calculate the relative contribution of the endmembers phytoplankton, POM_{estu}, macroalgae, marsh plants, and upland plants to invertebrate group diets. MixSIAR cannot handle unbalanced sample designs, and, thus, only samples that were analyzed for all four tracers were used in the model. Specifically, the low-glaciation site TUT was excluded from these analyses because of missing $\delta^{34}S$ data. TEFs help to clarify the difference among consumers and their dietary sources by accounting for the discrimination of stable isotopes during physiological processes (Caut et al. 2009; Philipps et al. 2014). MixSIAR incorporates TEFs into calculations of the proportion of source contributions by applying a fixed adjustment to the source values to adjust for physiological discrimination and then incorporates an uncertainty coefficient based on the standard deviation of those values. Because the taxon-specific TEFs of consumers in this present study were unknown, literature values of $\Delta\delta^{13}C = 0.75 \pm 0.11$‰ (Caut et al. 2009), $\Delta\delta^{15}N = 2.75 \pm 0.01$‰ (Caut et al. 2009), and $\Delta\delta^{34}S = 0.40 \pm 0.52$‰ (McCutchan et al. 2003) were used to account for discrimination in both invertebrate feeding groups. These TEF values were selected because they represent the calculated means of numerous estimates compiled from published studies.

The stable isotope compositions of phytoplankton and POM_{estu} samples were too similar to distinguish in mixing model analyses. Overlapping source signatures can hinder stable isotope mixing models from converging upon a unique solution, a problem often treated with methods such as source aggregation or the inclusion of informed priors (Brett 2014; Phillips et al. 2014). This issue was addressed in our model by aggregating phytoplankton and POM_{estu} (henceforth "POM_{mix}"). Overlap was still present between the new POM_{mix} endmember and macroalgae. However, there seemed sufficient variation of endmember position in isotope space among sites and discharge periods to warrant

further analysis given the use of informed priors on invertebrate diets (Supplement I, Table S1). Priors were obtained from gut content analysis of each invertebrate species using the methods of Lima-Júnior and Goitein (2001) and Moore and Semmens (2008). The intestinal tracts of invertebrates were first removed and lavaged with filtered seawater, contents were pipetted onto a gridded microscope slide, and components (phytoplankton cells, algal detritus, terrestrial detritus) were quantified when contacting a grid intersection; samples were then averaged within consumer groups for each discharge period.

All consumer models were run using JAGS software in the R package "R2jags" v0.6–1 (Su and Yajima 2021) and fitted using Markov Chain Monte Carlo sampling. The models consisted of three chains, run for 10^4 iterations, with a burn-in of 10^3, and a posterior thinning of 50. Model convergence was assessed using MixSIAR diagnostic Geweke and Gelman-Rubin tests. The information gained by using informed priors was considerable. Hellinger values, indicating the difference between model prior and posterior probability distributions, were higher, on average (Supplement I, Table S2), when compared to the uninformed mixing model, which suggests that the posterior distributions strongly diverged from the prior distributions. Furthermore, narrow posterior distributions of the final models indicated that the data were informative of the estimated consumer diets.

Watershed Characteristics

Watershed characteristics were calculated for use in distance-based redundancy analysis (dbRDA) to explain the watershed drivers of consumer stable isotope composition. Upstream characteristics were chosen that likely affect the variability in nearshore conditions from the river export of organic matter and nutrients to the coastal environment. These metrics included watershed area (km^2), mean slope (%), glacial coverage (% of watershed area), river flow length (km), and proportional coverage of vegetation (%) (Table 1). Metrics were derived from a digital elevation model (DEM) and multispectral imagery using ArcGIS 10.3. DEMs were obtained from the US Geological Survey Alaska Mapping Initiative interferometric synthetic aperture radar elevation dataset and SPOT 5 2.5-m multispectral imagery from the Alaska Statewide Mapping Initiative. Watershed area and glacial coverage were calculated using the *calculate geometry* function to compute summary statistics for each cell in the raster input. The slope of the terrestrial portion of each watershed was calculated using the *slope* function, which identifies the maximum rate of change from each map cell to its neighbor. River length was calculated using the *measure tool* on third-order streams, which measures the straight-line distance from each map cell to a user-designated point. Proportional coverage of vegetation was determined through *supervised classification*, in which groups of training pixels are chosen to create a signature file representative of landcover spectral reflectance.

Stream water chemistry was assessed for the concentration of organic and inorganic components of nitrogen, carbon, and total suspended solids (TSS). These were data acquired as part of a separate project and shared with the present study to provide context of upstream processes in the study catchments. As a result, water chemistry at each site was limited to these available parameters. Water samples were collected from the stream (upstream from the salt front) in 1-L clear bottles, filtered through a 0.4-µm Whatman GF/F filter, and sent to SGS Canada for analytical services. Material fluxes were calculated using specific discharge measurements from each river or, when discharge data were unavailable, freshwater discharge models for the GoA (Supplement I, Table S3; Beamer et al. 2017).

Watershed Drivers of Stable Isotope Composition and Trophic Niche Metrics

Watershed characteristics best-explaining consumer diets were identified using dbRDA in R package "vegan" v2.5–6 (Oksanen et al. 2019), which tested the significance of watershed characteristics on the response of consumer stable isotope composition. dbRDA applies multivariate multiple regression of principal coordinate axes on predictor variables to detect linear and nonlinear combinations of predictor variables that explain the greatest variability in a response dataset (Legendre and Anderson 1999). In this study, a global model, which included all variables listed in Table 1, was modified by removing variables deemed non-significant ($\rho > 0.05$) through ANOVA on dbDRA axes, to achieve a parsimonious model containing only significant terms. The models were not factored by the discharge period as insufficient data were available to maintain a balanced design. Percent glaciation was initially the primary driver of interest, as the conceptual foundation of the study used in study site selection, but it was highly correlated ($\rho > 0.7$) with numerous other, more specific parameters and was, thus, removed from the analysis (Supplement I, Table S4). It can be assumed, however, that those highly correlated parameters (e.g., river TSS) are themselves a response to glacial influence, and that some inferences to percent glaciation might still be made from the strength of these vectors during analysis. Euclidean distance measures were chosen for the model of each feeding group using the "vegan" rank-index function in R, and the model was built using the square root of dissimilarities to reduce negative eigenvalues.

Results

Source and Consumer Stable Isotope Values

A total of 351 invertebrate, 99 POM_{estu}, 13 phytoplankton, 451 macroalgal, and 366 vascular plant samples were analyzed for stable carbon and nitrogen isotope composition across the five Kachemak Bay sites, two years, and three discharge periods; 153, 30, 6, 131, and 89 samples, respectively, were also analyzed for stable sulfur isotopes (Table 2). The two consumer groups, respectively, differed significantly in stable isotope composition among glacial watershed sites (PERMANOVA Gr/De group: $F = 10.69$; $p = 0.001$, n = JAK:17, HAL:14, WOS:24, GRW:17; Su/FF group: $F = 21.27$, $p = 0.001$, n = JAK:20, HAL:12, WOS:25, GRW:24; Table 3), but not years or discharge period. Differences in consumers among sites were mostly ubiquitous among pairwise interactions (Supplement I, Table S5).

Consumer mean $\delta^{13}C$ values differed between feeding groups, with the Gr/De group ranging over 7.8 ‰ across all sites and periods from – 21.0 to – 13.2‰, and the Su/FF group ranging over 4.1‰ from – 20.2 to – 16.1‰ (Table 2; Fig. 2). Although mean $\delta^{13}C$ was higher for the Gr/De than the Su/FF group across sites, both groups exhibited a slight decrease in $\delta^{13}C$ with increasing glacial influence, with similar regression slopes, as indicated by a nonsignificant interaction effect between consumer $\delta^{13}C$ and feeding group (ANCOVA $F = 1.09$, $p = 0.297$, $n = 351$) (Fig. 2). There were no major differences or trends in consumer $\delta^{15}N$ or $\delta^{34}S$ among sites, years, or discharge periods.

An interest in this study was in assessing stable carbon isotope values as a characteristic biomarker of different primary producer sources. For the marine endmembers, stable isotope composition of POM_{mix} was significantly different among sites and discharge periods (PERMANOVA $F = 4.0$; $p = 0.005$ n = JAK:6, HAL:6, WOS:6, GRW:6; $F = 5.52$; $p = 0.001$, n = base:10, peak:10, post-peak:10, respectively; Table 3). The mean POM_{mix} $\delta^{13}C$ values

Table 3 PERMANOVA results of differences in the stable isotope composition of the grazer/detritivore (Gr/De) group, suspension/filter-feeding (Su/FF) group, and sources by Kachemak Bay site and discharge period (base, peak, post-peak)

Type	DF	SS	R^2	F	Pr(>F)
Gr/De					
Site	4	0.46	0.21	10.69	0.001
Flow period	2	0.01	0.01	0.99	0.436
Su/FF					
Site	4	0.04	0.32	21.27	0.001
Flow period	2	0.00	0.01	0.26	0.847
Phytoplankton					
Site	-	-	-	-	-
Flow period	64	0.39	0.61	49.32	0.001
POM_{mix}					
Site	4	0.04	0.15	4.00	0.005
Flow period	2	0.03	0.10	5.52	0.001
Macroalgae					
Site	4	0.44	0.14	17.87	0.001
Flow period	2	0.19	0.06	14.66	0.001
Marsh plant					
Site	4	0.11	0.11	7.14	0.001
Flow period	2	0.03	0.03	3.73	0.007
Upland plant					
Site	4	0.02	0.05	1.16	0.260
Flow period	2	0.08	0.22	17.25	0.001

Offshore phytoplankton were collected at one location and applied to all sites

PERMANOVA was conducted using multivariate isotope data (C, N, S) (see "Stable Isotope Mixing Models"). Differences are based on the Bray–Curtis dissimilarity of raw data

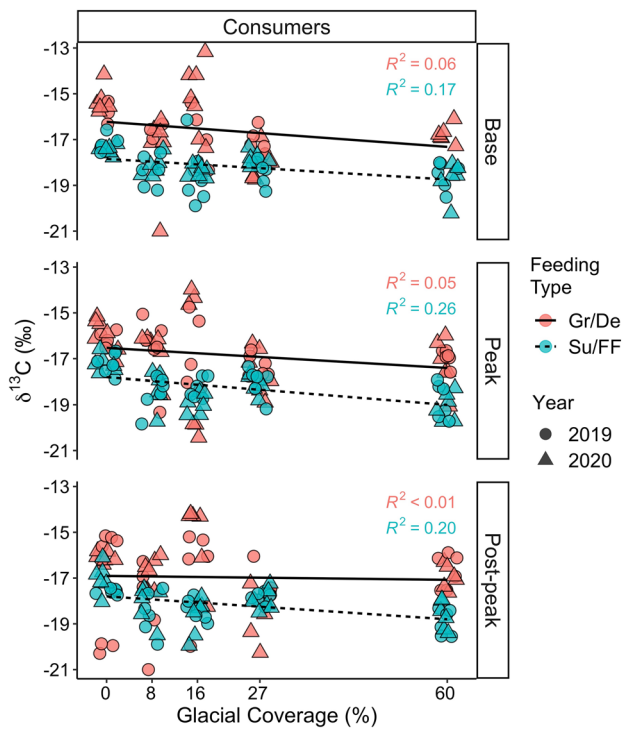

Fig. 2 $\delta^{13}C$ values (‰) by Kachemak Bay sampling site and discharge period (base, peak, post-peak) for consumer feeding groups. Jittered points represent individuals sampled; symbol color indicates feeding group; symbol shape indicates year sampled. Numbers associated with site names represent the percent glaciation of the watershed. Gr/De, grazers/detritivores; Su/FF, suspension/filter feeders. The black lines represent linear regressions of consumer $\delta^{13}C$ as a function of watershed glacier coverage, with regression R^2 values given in the plot, colored by feeding type

ranged over 2.2‰ from − 22.6 to − 20.4‰ across all sites and over 2.9‰ from − 22.7 to − 19.8‰ across discharge periods (Table 2, Fig. 3). Differences among sites were based on pairwise interactions of the non-glacial site JAK with other sites, and differences among discharge periods were based on the base flow pairwise comparison with the other two discharge periods (Supplement I, Table S5). The $\delta^{13}C$ composition of macroalgae also was significantly different among sites and discharge periods (PERMANOVA $F = 17.87$; $p = 0.001$, $n =$ JAK:36, HAL:14, WOS:40, GRW:41; $F = 14.66$; $p = 0.001$, $n =$ base:31, peak:10, post-peak: 31, respectively; Table 3), with mean $\delta^{13}C$ values ranging over 2.0 from − 19.7 to − 17.7‰ factored by site, and 3.5‰ from − 20.2 to − 16.7‰ factored by discharge period (Table 2, Fig. 3). Differences in macroalgae among sites and discharge periods were mostly ubiquitous among pairwise interactions (Supplement I, Table S6).

For the terrestrial endmembers, the $\delta^{13}C$ composition of marsh plants was significantly different among sites and discharge periods (PERMANOVA $F = 7.14$; $p = 0.001$, $n =$ JAK:16, HAL:12, WOS:13, GRW:12; $F = 3.73$, $p = 0.007$, $n =$ base:12, peak:10, post-peak:31, respectively; Table 3), with mean $\delta^{13}C$ values ranging over 1.3‰ from − 25.9 to 24.6‰ across sites, and over 4.1‰ from − 27.5 to − 23.4‰ across discharge periods (Table 2, Fig. 3). Differences among sites involved pairwise comparisons including the non-glacial JAK or low-glacial TUT sites, and differences among discharge periods involved peak and post-peak flow comparisons (Supplement I, Tables S5 and S6). The $\delta^{13}C$ composition of upland plants was only significantly different among discharge periods (PERMANOVA $F = 17.25$; $p = 0.001$, $n =$ base:10, peak:10, post-peak:16; Table 3), with mean $\delta^{13}C$ values ranging over 3.3‰ from − 30.3 to − 27.0‰ (Table 2; Fig. 3). Differences among discharge periods were ubiquitous among pairwise comparisons (Supplement I, Table S6).

Estimated Source Contributions to Invertebrate Consumers

Consumer stable isotope ratios varied among sites but were distinctly positioned by feeding group within the marine source distributions (Fig. 4). Model-estimated dietary contributions varied between consumer groups but were principally

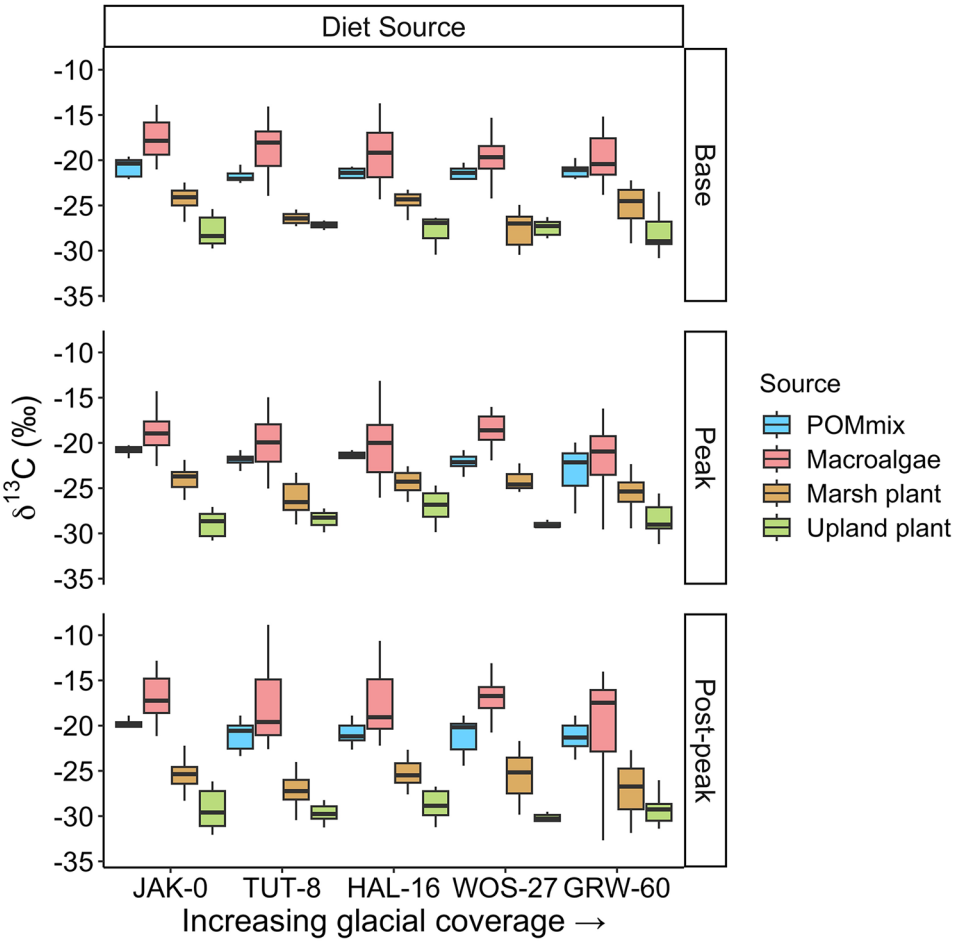

Fig. 3 $\delta^{13}C$ values (‰) by Kachemak Bay sampling site and discharge period (base, peak, post-peak) for diet sources included in stable isotope mixing models. Box color indicates diet source (POM_{mix}, macroalgae, marsh plant, upland plant) and numbers associated with site names represent the percent glaciation of the watershed. Boxes represent the interquartile range, bold lines within boxes mark the range median, and whiskers represent the lower and upper extreme values

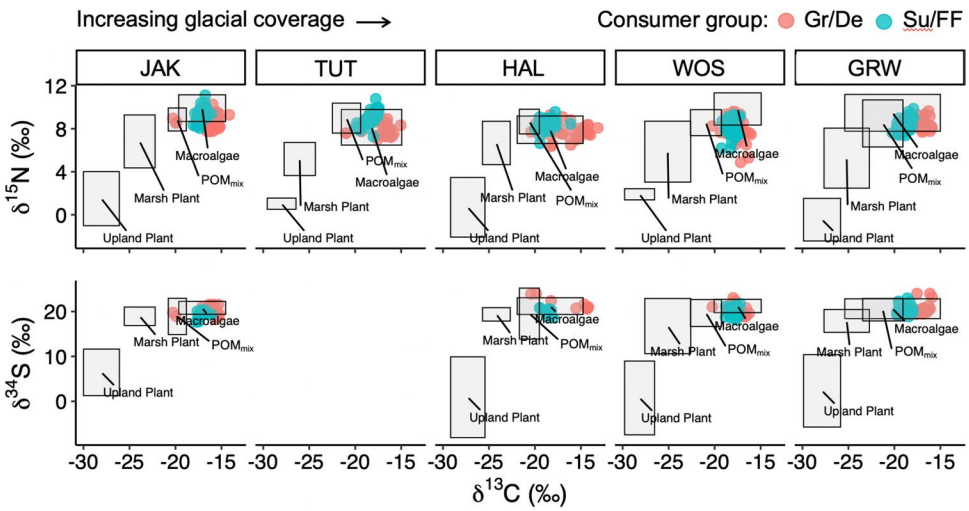

Fig. 4 Stable isotope biplots of $\delta^{13}C$ versus $\delta^{15}N$, and $\delta^{13}C$ versus $\delta^{34}S$ values (‰) of individual samples by consumer group in Kachemak Bay. Data points are individual samples; symbol color indicates consumer group; all consumers are positioned after accounting for trophic discrimination factors (C = 0.75 ± 0.11, N = 2.75 ± 0.10, S = 0.40 ± 0.52). Shaded boxes represent the position and distribution (mean ± 1SD) of diet sources (POM_{mix}, macroalgae, marsh plants, upland plants). No sulfur stable isotope values were available for the Tutka (TUT) site. Gr/De, grazers/detritivores; Su/FF, suspension/filter feeders. This plot was not factored by discharge period due to prevailing themes among periods: consumers were always within the overall resource space and specifically located in the marine source boxes

marine, as indicated by the median point estimates of posterior distributions, considering that the POM_{mix} source is almost entirely of marine origin (Table 4, Fig. 5). For the Gr/De group, POM_{mix} was the predominant food source and contributed 38–40% during base flow and 54–72% during peak and post-peak flow periods. Macroalgal contributions were second highest but varied among periods with 51–54% during base flow, 14–17% during peak flow, and 32–35% during post-peak flow. Marsh and upland plant contributions to Gr/De diet were low and ranged from 3 to 7% and 3 to 5%, respectively, and were mostly consistent across sites and discharge periods. Among the discharge periods, overlap in the posterior distributions of marine diet contributions to the Gr/De group occurred during the base and peak-flow periods, yet diverged distinctly during peak flow and post-peak flow periods, where there was a greater distinction between macroalgal and influence of POM_{mix} (Fig. 5) and an elevated contribution of terrestrial sources relative to the base flow period. Diet contributions of the Su/FF group were also dominated by POM_{mix}, contributing 59–71% across sites and discharge periods with the greatest POM_{mix} contribution estimates during peak flow. Macroalgal contributions ranged from 22 to 31% and were mostly unchanging among sites and flow periods. Terrestrial contributions to Su/FF diets ranged from 2 to 6%, with similar contributions across sites and discharge periods. Unlike the Gr/De group, posterior distributions of all diet contributions to the Su/FF group were distinct, with the only overlap between the two terrestrial sources and with similar patterns among discharge periods.

Watershed Drivers of Stable Isotope Composition

Of the distinct watershed characteristics contributing to each study site (Table 1), there were three watershed characteristics that best explained the variability of the stable isotope composition of Gr/De which were percent vegetation, river length, and ruggedness. The four drivers best explaining the variability of the Su/FF group were the same as those of the Gr/De group with percent vegetation, river length, and ruggedness, but also included TSS.

Overall, these drivers explained 49.44% and 55.01% of the total variance in Gr/De and Su/FF group diets, respectively (Fig. 6). For the Gr/De group, dbRDA Axis 1 explained the greatest variance (90.51% of fitted, 44.75% total explained variance) and was most associated with river length ($\rho = 0.47$), then percent vegetation ($\rho = 0.20$), and ruggedness ($\rho = 0.02$), while dbRDA Axis 2 explained less variance (7.5% of fitted, 3.71% total explained variance) and was associated negatively first with river length ($\rho = -0.39$), then percent vegetation ($\rho = -0.22$), and then ruggedness ($\rho = -0.14$). For the Su/FF group, dbRDA Axis 1 also explained the greatest variance (78.83% of fitted, 40.24% total) and was most associated negatively with percent vegetation ($\rho = -0.78$), then positively with TSS ($\rho = 0.62$) and ruggedness ($\rho = 0.58$), and then negatively with river length ($\rho = -0.14$). dbRDA Axis 2 also explained a lower proportion of variance (15.34% of fitted, 7.83% total) and was most associated with river length ($\rho = 0.28$), then TSS ($\rho = 0.22$), ruggedness ($\rho = 0.18$), and lastly, percent vegetation ($\rho = 0.11$).

Table 4 Invertebrate consumer groups diet median and interquartile range (IQR) estimates of proportional source contributions, separated by Kachemak Bay site and discharge period (base, peak, post-peak), based on stable isotope mixing model results

Type	Site	Source	Base flow		Peak flow		Post-peak flow	
			Median	IQR	Median	IQR	Median	IQR
Gr/De	JAK-0	POM_{mix}	0.39	0.07	0.72	0.08	0.59	0.07
		Macroalgae	0.54	0.07	0.17	0.07	0.32	0.06
		Marsh plant	0.04	0.03	0.06	0.04	0.05	0.03
		Upland plant	0.03	0.02	0.04	0.03	0.04	0.02
	HAL-16	POM_{mix}	0.38	0.06	0.73	0.08	0.54	0.06
		Macroalgae	0.55	0.07	0.15	0.06	0.35	0.06
		Marsh plant	0.04	0.03	0.07	0.04	0.06	0.03
		Upland plant	0.03	0.02	0.04	0.03	0.05	0.03
	WOS-27	POM_{mix}	0.41	0.07	0.75	0.08	0.58	0.07
		Macroalgae	0.51	0.07	0.14	0.06	0.32	0.06
		Marsh plant	0.03	0.02	0.06	0.04	0.06	0.03
		Upland plant	0.04	0.03	0.04	0.03	0.04	0.02
	GRW-60	POM_{mix}	0.38	0.07	0.75	0.08	0.57	0.06
		Macroalgae	0.54	0.06	0.14	0.06	0.33	0.06
		Marsh plant	0.04	0.02	0.06	0.04	0.05	0.03
		Upland plant	0.03	0.02	0.05	0.03	0.04	0.02
Su/FF	JAK-0	POM_{mix}	0.61	0.06	0.68	0.06	0.62	0.06
		Macroalgae	0.30	0.06	0.26	0.06	0.28	0.06
		Marsh plant	0.03	0.02	0.03	0.02	0.05	0.03
		Upland plant	0.05	0.02	0.02	0.02	0.04	0.02
	HAL-16	POM_{mix}	0.59	0.06	0.68	0.06	0.59	0.07
		Macroalgae	0.31	0.06	0.25	0.06	0.29	0.06
		Marsh plant	0.03	0.02	0.04	0.03	0.06	0.03
		Upland plant	0.06	0.03	0.03	0.02	0.05	0.03
	WOS-27	POM_{mix}	0.61	0.06	0.69	0.06	0.61	0.07
		Macroalgae	0.30	0.06	0.23	0.06	0.28	0.06
		Marsh plant	0.03	0.02	0.04	0.03	0.06	0.03
		Upland plant	0.06	0.02	0.04	0.02	0.05	0.02
	GRW-60	POM_{mix}	0.61	0.07	0.71	0.06	0.62	0.07
		Macroalgae	0.30	0.06	0.22	0.06	0.28	0.06
		Marsh plant	0.03	0.02	0.03	0.02	0.05	0.03
		Upland plant	0.06	0.03	0.03	0.02	0.04	0.02

The value associated with site name represents the percent glacial cover of the watershed. Site TUT-8 was excluded, because of missing sulfur stable isotope values

Gr/De grazers/detritivores, *Su/FF* suspension /filter feeders

Overlap in dbRDA space among sites occurred for both consumer groups (Fig. 6). Visually, the Gr/De group expressed little overlap among sites, with no common overlap area shared among all site ellipses due to the distant position of the HAL site. In general, Gr/De group sites were positioned along dbRDA Axis 1 in order of slope, with HAL (greatest slope) positioned left, decreasing to GRW (lowest slope), positioned right. Ellipses of the Su/FF group were more evenly distributed throughout dbRDA space with more vertically stretched ellipse orientations. The Su/FF group expressed greater overlap among site confidence ellipses ($\alpha = 0.05$), with all sites sharing some common dbRDA space. The horizontal separation of sites along Axis 1 was largely driven by percent vegetation and ruggedness, which positioned sites towards the negative side of Axis 1, and TSS and river length, which pushed sites towards the positive side of Axis 1. In general, this reflected positioning along dbRDA Axis 1 from left to right in order of increasing glacial influence, except for HAL, which was positioned to the far right past the highest glaciation site, GRW. Ellipse areas of all Su/FF group sites also were oriented along dbRDA Axis 2, despite the lower explanatory power and no specific drivers associated with this axis.

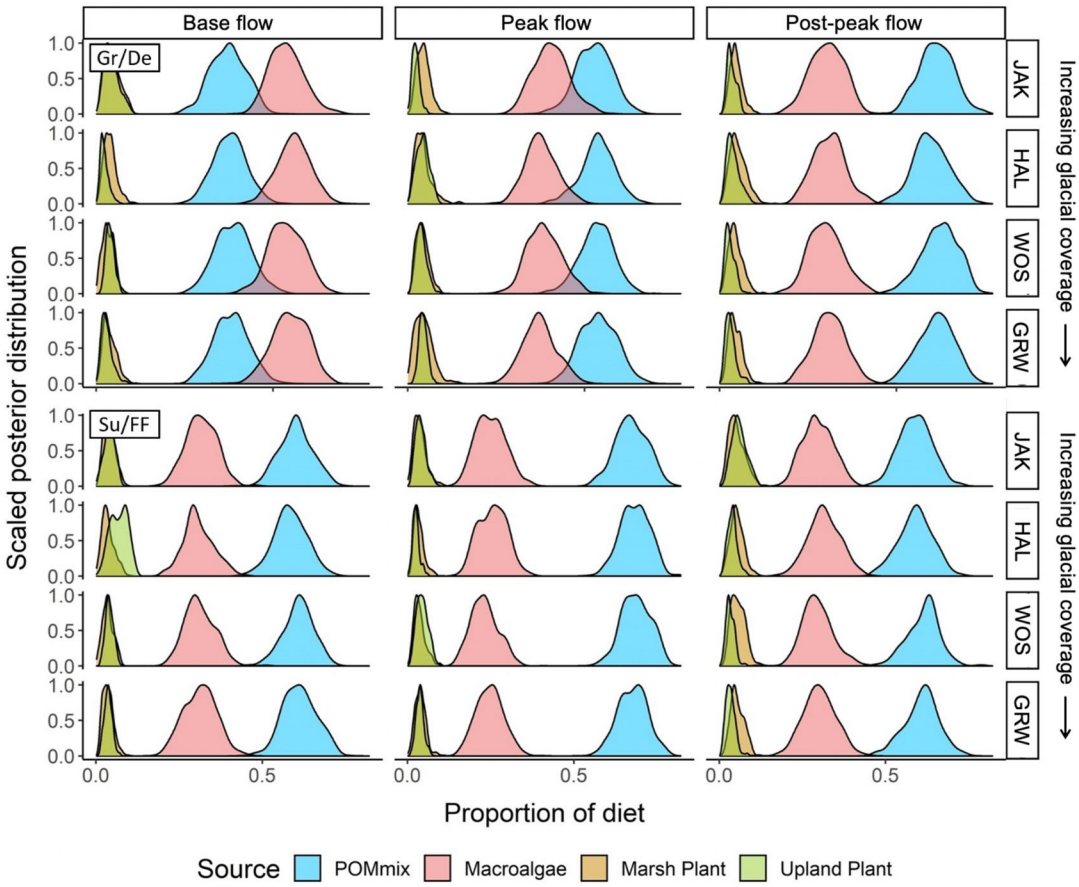

Fig. 5 Scaled posterior density distributions of proportional diet source contributions to consumer groups (top: Gr/De group, bottom: Su/FF group) by Kachemak Bay site and discharge period (base, peak, post-peak). Distribution color indicates diet source (POM_{mix}, Macroalgae, Marsh plant, Upland plant). Numbers associated with site names represent the percent glaciation of the watershed. Site TUT-8 was excluded because no sulfur stable isotope values were available. Gr/De, grazers/detritivores; Su/FF, suspension/filter feeders

Discussion

The overall goal of this study was to investigate the effects of glacial influence on the diets of nearshore invertebrates, specifically the use of terrestrial subsidies, by assessing shifts in food resource use and trophic niche space over a range of watersheds with different glaciation levels and across seasonal discharge regimes. In contrast to a recent surge in the literature supporting the substantial use of terrestrial resources in marine invertebrate diets, the results of this study indicate that consumer diets were largely decoupled from terrestrial sources. Both Gr/De and Su/FF invertebrate taxa fed predominantly on marine sources across glacial influence and discharge regimes, although Gr/De relied more prominently on macroalgae and Su/FF on POM. While there were differences in resource space occupied by the two consumer groups, there were few patterns consistent with overall glacial influence or discharge period for either group. In contrast, drivers of consumer stable isotope composition were shown in our models to associate with unique watershed characteristics rather than linearly with glaciation. This combination of results suggests that terrestrial watershed characteristics may influence marine primary producers in the study system, but dietary augmentation with terrestrial resources may not be necessary for marine invertebrate consumers in a highly productive marine system like Kachemak Bay.

Stable Isotope Composition of Consumers

The enrichment of the Gr/De group in ^{13}C relative to the Su/FF group indicates reliance on different food sources and is consistent with diet differences between the groups in other nearshore systems. For example, the typical $\delta^{13}C$ values of grazing limpets of the genus *Lottia* are often 1–2‰ higher than the suspension-feeding genus *Balanus* when examined across the geographic spread from Puget Sound, Washington to the Lower Cook Inlet, Alaska (Ruesink et al. 2014; Siegert

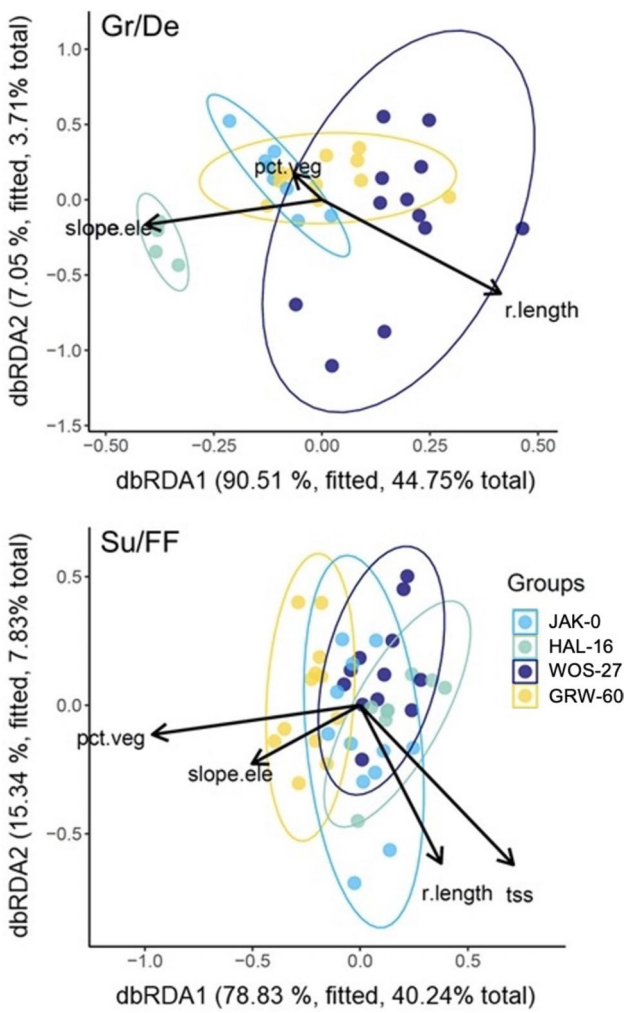

Fig. 6 Distance-based redundancy analysis (dbRDA) ordination of the multivariate stable isotope composition of consumer feeding groups (top: Gr/De group, bottom: Su/FF group) by Kachemak Bay site. Data points indicate individual consumer samples; colors indicate site; ellipses indicate 95% confidence interval; vector length is relative to significant predictor strength; axis values in parenthesis show fitted and total explained variance. Predictor variables that were selected as significant included percent vegetations (pct.veg), ruggedness (slope.ele), river length (r.length), and river total suspended solids (TSS). Site TUT-8 was excluded because no sulfur stable isotope values were available. Gr/De, grazers/detritivores; Su/FF, suspension/filter feeders

et al. 2022), consistent with grazing on an isotopically heavier food source. The taxa within the Gr/De group sampled in this study (*Littorina* spp. and *Lottia* spp.) are known to feed upon a mix of red, green, and brown algae (Kozloff 1996). The range of macroalgal $\delta^{13}C$ values was larger than any other diet source in this study, reflecting the wide range of macroalgal stable isotope values driven by environmental conditions, their thallus forms, growth rates, and carbon concentrating mechanisms (Wiencke and Fischer 1990; France 1995; Giordano et al. 2005). While $\delta^{13}C$ isotope values of macroalgae within this study ranged from − 10 to − 31‰, macroalgal isotopic variability may be even larger than demonstrated here, where we only considered four common intertidal macroalgae; the total diversity of macroalgae present in the system is considerable (Konar et al. 2010). Gr/De consumers were only positioned within the − 13‰ to − 21‰ range, indicating their preferential feeding on macroalgae with higher $\delta^{13}C$ values such as many brown algae (e.g., Siegert et al. 2022). An alternative, unsampled carbon source of high $\delta^{13}C$ values could be microphytobenthos (MPB). MPB is an organic film in marine systems consisting of diverse microalgal assemblages and microorganisms such as cyanobacteria, diatoms, flagellates, and settled macroalgal spores as well as trapped detrital matter (MacIntyre et al. 1996). This biofilm covering rocky substrate is an accessible food source for grazing organisms. Although difficult to measure, previous studies in Alaska have reported mean MPB $\delta^{13}C$ values of − 16.9 ± 1.2‰ (McTigue and Dunton 2017). This overlaps well with the Gr/De consumer values and is similar to the higher range of macroalgal $\delta^{13}C$ values sampled in this study and, thus, poses as another viable endmember to explain the isotope range of the Gr/De group.

The taxa within the Su/FF group (*Balanus* spp. and *Mytilus trossulus*) generally feed on a mix of phytoplankton, small zooplankton, and POM. POM is a mixed source that combines non-living matter from the cellular components of plankton, bacteria, and protists with detrital components from plants, algae, and other marine organisms (Volkman and Tanoue 2002). Especially the large portion of microalgae in POM leads to lower $\delta^{13}C$ values compared to macroalgae (Lowe et al. 2014); the $\delta^{13}C$ values of POM_{mix} in this study were often 1–3‰ lower than macroalgae, despite the general overlap of the two sources in stable isotope space (Fig. 4). This greater ingestion of POM compared to macroalgae was reflected in the smaller $\delta^{13}C$ values of the Su/FF than the Gr/De group. Still, macroalgal detritus has been shown to contribute to suspension-feeding bivalve diets (Duggins et al. 1989; Howe and Simenstad 2015; Both et al. 2020), particularly during periods (Langdon and Newell 1990) or locations (Siegert et al. 2022) of low phytoplankton abundance.

Both Gr/De and Su/FF groups showed similar decreasing trends of $\delta^{13}C$ values with increasing percent watershed glaciation during all discharge periods. These patterns could be explained by either a change in diet or a glacially driven decrease in the $\delta^{13}C$ value of a diet source across watersheds. There is no indication of diet change with watershed glaciation in our mixing model estimates of diets. In contrast, the $\delta^{13}C$ values of autotrophs (e.g., phytoplankton, macroalgae) are determined by uptake fractionation during photosynthesis (Keller and Morel 1999), which is influenced by cell physiology (Popp et al. 1998), ambient environmental conditions (Burkhardt et al. 1999), and the availability of

dissolved inorganic carbon (DIC) (Sharkey and Berry 1985; Lammers et al. 2017). The mobilization of geogenic DIC is especially high in high-latitude, watersheds with glacial coverage due to physical weathering associated with glacial movement (Tranter and Wadham 2013), and the DIC yield is often greater in watersheds of higher glacial coverage relative to those of lower or no coverage (Jenckes et al. 2022). This pattern is consistent with the positive relationship between the flux of DIC and the glacial coverage of watersheds in this study (Supplement I, Table S1). Correspondingly, the greater flux of DIC from watersheds with glacial coverage is likely to decrease the $\delta^{13}C$ values of marine phytoplankton because carbon stable isotope discrimination in most marine algae is inversely related to the concentration of DIC in the aqueous pool (Sharkey and Berry 1985). These results suggest that the slight decrease in POM_{estu} $\delta^{13}C$ values may stem from differences in the $\delta^{13}C$ of local, estuarine phytoplankton that were unaccounted for in our offshore, marine phytoplankton samples.

Estimated Source Contributions to Invertebrate Consumers

Mussels, barnacles, limpets, and periwinkles are among the most ubiquitous organisms in rocky intertidal systems worldwide, often characterizing community zonation patterns (Stephenson and Stephenson 1949). However, it should be noted that they are not fully representative of all feeding groups in an ecosystem and may be biased towards consuming marine resources over terrestrial when compared to other consumers. Still, the highly similar modeled diet contributions of POM_{mix}, macroalgae, and terrestrial plants across sites to both feeding groups suggest that these diet sources are consumed in similar proportions irrespective of feeding group and glacial coverage of the watershed. It was hypothesized that the terrestrial source contribution to consumer diets would vary among sites and discharge periods, considering that discharge volume and composition were expected to have higher terrestrial exports in watersheds with higher glacial cover and during peak discharge, which would influence the available resource pool. However, contrary to that expectation, the modeled proportion of terrestrial contribution to both feeding groups' diets was minor (7–10%) and consistent across discharge periods. These results suggest that the temporal uncertainty associated with tissue turnover and informative prior choice is minimal. Additionally, the inclusion of small amounts of terrestrial components in modeled consumer diets could at least in part be an artifact of the model because all sources included in the model will be attributed by default to some level of contribution (Parnell et al. 2013; Phillips et al. 2014). It is also possible that the prevalence of terrestrial OM was underestimated in these models because the endmembers used in the models may not represent all possible terrestrial sources available to consumers. Wetlands and peat bogs are common contributors of OM_{terr} to river systems in this region but were not included in this study due to their minimal presence in the studied watersheds (1–5% areal coverage). Furthermore, we used live land plants as endmembers because they commonly grew along waterways and coastlines and were observed in the waters and shorelines of the study sites. Fresh plant material differs from riverine POM, which ultimately is the degraded plant material transported in rivers to the coastal system. During this transport, the fractionation associated with degradation and mixing with soil organic matter can result in a ~ 2‰ increase in the $\delta^{13}C$ values of riverine POM by the time it is discharged into the ocean (Fiers et al. 2019). $\delta^{13}C$ values of riverine POM in glacially influenced systems in Southeast Alaska were − 28‰ (Whitney et al. 2018), a value that overlaps with those of the upland plants in our study. While we do not have riverine POM carbon isotope data to include in the mixing model, the potential increase in $\delta^{13}C$ would still position the riverine POM outside the trophic niche space of the consumers in this study (Fig. 4), although the calculated proportion of terrestrial matter in the consumer diet may have been slightly higher.

Marine or predominantly marine sources (macroalgae, POM_{mix}) contributed substantially (~ 90% combined sources) to the modeled diets of both feeding groups across space and time. The consistently high proportion of marine sources in consumer diets may represent a preference for higher-quality food derived from marine environments. Marine algae (macroalgae and phytoplankton) are more nutritious relative to terrestrial plant litter, in part due to a higher content of polyunsaturated fatty acids (Guo et al. 2016) and the absence of lignocellulosic structural compounds found in terrestrial plants (Wells et al. 2017). Thus, phytoplankton and macroalgae are evidently a major source of nutrition for these organisms. The use of a diverse source array of macroalgae, phytoplankton, and POM_{mix} by consumers aids in their resilience to the loss of, or variability in, a particular food source and contributes to ecosystem stability (Rooney and McCann 2012; Siegert et al. 2022). This is exemplified by the seasonal patterns in resource use by both feeding groups, where their diets shifted to incorporate less macroalgae and more POM_{mix} during the peak flow period. The relative availability of these resources is subject to the sourcing and transport characteristics of seasons, such that light limitation of phytoplankton contributing to seasonal POM_{mix} blooms and fragmentation of macroalgae from winter hydrodynamics (frequent and intense weather) may favor the prevalence of perennial macroalgal sources in spring over POM_{mix}. Conversely, high phytoplankton abundance and stable summer weather may favor the incorporation of

phytoplankton into organic aggregates, while freshwater discharge facilitates algal flocculation (Lee et al. 2019) and transports drift macroalgae offshore.

Sufficient availability of these marine organic matter sources may reduce the need for consumers to supplement their diets with lower-quality terrestrial resources. This idea is in line with optimal foraging theory, where the quality of a subsidy is important to the foraging strategies of animals, because they seek to optimize their digestible intake (forage quality), while minimizing the energetic cost of finding and handling food (Pyke 1984). Also, consumer life history traits (e.g., breeding success) are directly related to the availability of preferred food resources (Österblom et al. 2008) and, thus, could be negatively impacted by the reduced nutritional value of critical diet items. Kachemak Bay is a highly productive embayment (Chester and Larrance 1981), characterized by high macroalgal diversity and abundance (Konar et al. 2010), high macroalgal growth rates (Spurkland and Iken 2012), and high phytoplankton production (Griffiths et al. 1982). Given that these marine resources seem plentiful, it is plausible that they are sufficient to be the primary food resources for these consumers. OM_{terr} is generally used to a lesser extent in marine food webs unless access to autochthonous food items (e.g., macroalgae or phytoplankton) is hindered or limited (Fairbanks et al. 2018; Ray et al. 2018). Several studies have demonstrated that the use of OM_{terr} by marine consumers declines with distance from the freshwater source in coastal ecosystems (Bell et al. 2016; McMahon et al. 2021; Ray et al. 2018) or between the less productive upper and more productive lower continuums of estuaries (Cloern et al. 2017). In other systems such as arctic lagoons, marine OM use in food webs is often temporally linked to the duration of ocean connectivity (Fraley et al. 2021), such as seasonally "open" and "closed" phases of these lagoons (Dunton et al. 2012; Connelly et al. 2015). Kachemak Bay has a consistent connection to the open ocean (Johnson 2021) and, thus, oceanic endmembers. With great tides to facilitate flushing and transport, it likely supplies nearshore ecosystems with plentiful high-quality marine OM, regardless of the current strength of freshwater discharge.

Watershed Drivers of Consumer Stable Isotope Composition

Terrestrial sources only constituted a small portion of consumer diets, but the flux of terrestrial materials can still be important for coastal food webs. The supply of OM_{terr} to the coastal environment is governed by the composition of terrestrial characteristics, including vegetation, soils, lithology (Tiwari et al. 2017), and the watershed attributes that contribute to their mobilization and transport, such as hydrologic processes and catchment structure (Godsey et al. 2009). As a result, the OM_{terr} available to different invertebrate feeding types uniquely varies relative to the contributing watershed's source and transport attributes. The dbRDA model results indicated that the two feeding groups were associated with overall similar watershed drivers in this study system, yet, with different responses to these drivers. Specifically, the Gr/De group's stable isotope composition was regulated primarily by factors associated with transport (ruggedness) and sourcing (river length), while the Su/FF group was regulated primarily by factors associated with sourcing (TSS, percent vegetation).

OM_{terr} influx can stimulate coastal productivity through pathways other than direct ingestion by primary consumers. For example, the Gr/De groups' stable isotope composition was driven most by river length and ruggedness. Gr/De at sites with shorter streams (JAK, GRW) were distinct (higher $\delta^{13}C$ values) from those at sites with longer streams (HAL, WOS; lower $\delta^{13}C$ values). This may reflect the available carbon stocks stored in river floodplains, which contain most of the carbon found in most river corridors (Dunne et al. 1998; Sutfin et al. 2016). Once mobilized, these organic and inorganic materials stimulate the growth of heterotrophic bacteria in the nearshore estuary (Sutfin et al. 2016; Xu et al. 2018). Incidentally, the Gr/De group may consume heterotrophic bacteria assimilated within periphytic algae (Haglund and Hillebrand 2005), which could influence consumer $\delta^{13}C$ values when consumed based on the carbon source used in microbial respiration (Jennings et al. 2017). Furthermore, inorganic materials from the riverine pulse may act as ballast to organic marine aggregates (e.g., marine snow) suspended in the coastal water column and deposited into intertidal regions for consumption by the Gr/De group (Ross et al. 2022).

The Su/FF group was more prominently affected by the factors related to sourcing (TSS and percent vegetation). TSS is the chief export of mountainous watersheds and represents the amalgamation of the rugged land surface, topographically limited vegetation, short fluid transit times, and glacial erosion (Anderson 2005; Lafrenière and Sharp 2005; Wheatcroft et al. 2010; Jenckes et al. 2023). This relationship between Su/FF stable isotope composition and the TSS flux most likely represents intermediate pathways, such as marine phytoplankton responding to the input of nutrients and other trace minerals from the rivers (Arrigo et al. 2017). This nutrient input can result in a large proportion of nutrients available for uptake by phytoplankton, which serves as a key food source for the Su/FF group.

Interpretation of the percent vegetation vector for both feeding groups is less straightforward. In theory, it may represent a variety of processes, such as the direct subsidy of vegetal detritus to consumer diets, the enhancement of intermediate production of heterotrophic bacteria, or the control of vegetation on the transport of particulates in watercourses. Firstly, vegetal detritus as a subsidy to diets was unsupported

in the mixing model analysis. Second, heterotrophic bacteria might influence consumer stable isotope values through the enrichment of their diet sources—bacterial degradation preferentially uptakes lighter isotopes over heavier forms—or by increasing the $\delta^{15}N$ of consumers through direct consumption because of the added trophic step introduced (Bell et al. 2016). There were no apparent differences in the $\delta^{15}N$ of either group among sites (Fig. 4, Table 2) and, thus, no clear evidence of the influence of heterotrophic bacteria on the food chain. However, a lengthened food chain would rely on heterotrophic bacteria as a relatively consistent food resource for the consumers. While we did not see an increase in $\delta^{15}N$, this could be obscured by a lag effect in consumer $\delta^{15}N$ values based on consumer tissue turnover times that we may not have captured with our sampling strategy. Lastly, the site-specific confidence ellipses for Su/FF were generally ordered by glaciation, except for the HAL site, which supports the opposing influence of TSS in stream water, and the effect of percent vegetation in reducing the delivery of solids to streams.

Conclusion

This study aimed to investigate the effects of glacial influence on the diets of nearshore invertebrates, represented by Gr/De and Su/FF trophic groups. The negative relationship between the $\delta^{13}C$ values of consumers and glacial influence is likely linked to the physiology of diet sources, where stable isotope fractionation processes of temporally dependent sources (i.e., phytoplankton, macroalgae) are influenced by local conditions, such as nutrient and DIC inputs (Calleja et al. 2017). Presumably, such processes would be expressed in shifts in the stable isotope values of a diet source; however, in the case of sources characterized by fast turnover times (i.e., phytoplankton), such trends may be obscured by high temporal variability. As a result, trends in the carbon stable isotope ratios of taxa in this study could be a product of variability in their marine diet sources, which can be influenced by glacial discharge, but their diet is decoupled from direct terrestrial intake. These findings contrast several other studies in the North Pacific region that found significant terrestrial matter in nearshore consumer diets (e.g., Howe and Simenstad 2015; Whitney et al. 2018). It is possible that the high productivity of the Kachemak Bay study system leads to an abundance of highly labile marine food sources, rendering the diet augmentation with less labile terrestrial matter unnecessary. These results corroborate assessments made in nearby, productive Prince William Sound, Alaska (Arimitsu et al. 2018) and elsewhere in productive rocky intertidal systems (Corbisier et al. 2006), which also suggest that terrestrial carbon is not readily incorporated into marine food webs despite its availability. These systems are similarly characterized by high faunal biomass and complex trophic structures, which indicate ecosystem maturation in response to the increasing ratio of marine to terrestrial organic matter sources (Zaborska et al. 2018). The congruency of findings between marine source-dominated food webs in highly productive areas and the use of terrestrial subsidies in systems that presumably have lower productivity supports the notion that consumers will select higher-nutrition OM sources when available.

Supplementary Information The online version contains supplementary material available at https://doi.org/10.1007/s12237-023-01277-9.

Acknowledgements We are indebted to Dr. Brenda Konar (University of Alaska Fairbanks) for her guidance and constructive comments on this manuscript.

Funding This work was part of the Alaska National Science Foundation (NSF) Established Program to Stimulate Competitive Research (EPSCoR) "Fire and Ice: Navigating Variability in Boreal Wildfire Regimes and Subarctic Coastal Ecosystems (F&I)" project, funded by the NSF (Award Number 1757348).

Open Access This article is licensed under a Creative Commons Attribution 4.0 International License, which permits use, sharing, adaptation, distribution and reproduction in any medium or format, as long as you give appropriate credit to the original author(s) and the source, provide a link to the Creative Commons licence, and indicate if changes were made. The images or other third party material in this article are included in the article's Creative Commons licence, unless indicated otherwise in a credit line to the material. If material is not included in the article's Creative Commons licence and your intended use is not permitted by statutory regulation or exceeds the permitted use, you will need to obtain permission directly from the copyright holder. To view a copy of this licence, visit http://creativecommons.org/licenses/by/4.0/.

References

Abrantes, K., J. Semmens, J. Lyle, and P. Nichols. 2012. Normalisation models for accounting for fat content in stable isotope measurements in salmonid muscle tissue. *Marine Biology* 159: 57–64. https://doi.org/10.1007/s00227-011-1789-1.

Anderson, S.P. 2005. Glaciers show direct linkage between erosion rate and chemical weathering fluxes. *Geomorphology* 67 (1–2 SPEC. ISS.): 147–157. https://doi.org/10.1016/j.geomorph.2004.07.010.

Arimitsu, M.L., K.A. Hobson, D.N. Webber, J.F. Piatt, E.W. Hood, and J.B. Fellman. 2018. Tracing biogeochemical subsidies from glacier runoff into Alaska's coastal marine food webs. *Global Change Biology* 24 (1): 387–398. https://doi.org/10.1111/gcb.13875.

Arnosti, C. 2011. Microbial extracellular enzymes and the marine carbon cycle. *Annual Review of Marine Science* 3: 401–425. https://doi.org/10.1146/annurev-marine-120709-142731.

Arrigo, K.R., G.L. van Dijken, R.M. Castelao, H. Luo, ÅK. Rennermalm, M. Tedesco, T.L. Mote, H. Oliver, and P.L. Yager. 2017. Melting glaciers stimulate large summer phytoplankton blooms in southwest Greenland waters. *Geophysical Research Letters* 44 (12): 6278–6285. https://doi.org/10.1002/2017GL073583.

Beamer, J.P., D.F. Hill, D. McGrath, A. Arendt, and C. Kienholz. 2017. Hydrologic impacts of changes in climate and glacier extent in the Gulf of Alaska watershed. *Water Resources Research* 53: 7502–7520. https://doi.org/10.1002/2016WR020033.

Bell, L.E., B.A. Bluhm, and K. Iken. 2016. Influence of terrestrial organic matter in marine food webs of the Beaufort Sea shelf and slope. *Marine Ecology Progress Series* 550: 1–24. https://doi.org/10.3354/meps11725.

Berglund, J., U. Müren, U. Båmstedt, and A. Andersson. 2007. Efficiency of a phytoplankton-based and a bacteria-based food web in a pelagic marine system. *Limnology and Oceanography* 52 (1): 121–131. https://doi.org/10.4319/lo.2007.52.1.0121.

Both, A., C.J. Byron, B. Costa-Pierce, C.C. Parrish, and D.C. Brady. 2020. Detrital subsidies in the diet of *Mytilus edulis*; macroalgal detritus likely supplements essential fatty acids. *Frontiers in Marine Science* 7 (12): 1–22. https://doi.org/10.3389/fmars.2020.561073.

Brett, M.T. 2014. Resource polygon geometry predicts Bayesian stable isotope mixing model bias. *Marine Ecology Progress Series* 514: 1–12. https://doi.org/10.3354/meps11017.

Burkhardt, S., U. Riesbell, and I. Zondervan. 1999. Effects of growth rate, CO_2 concentration, and cell size on the stable carbon isotope fractionation in marine phytoplankton. *Geochimica Et Cosmochimica Acta* 63 (22): 3729–3741. https://doi.org/10.1016/S0016-7037(99)00217-3.

Calleja, M.L., P. Kerhervé, S. Bourgeois, M. Kędra, A. Leynaert, E. Devred, M. Babin, and N. Morata. 2017. Effects of increase glacier discharge on phytoplankton bloom dynamics and pelagic geochemistry in a high Arctic fjord. *Progress in Oceanography* 159: 195–210. https://doi.org/10.1016/j.pocean.2017.07.005.

Canuel, E.A., and A.K. Hardison. 2016. Sources, ages, and alteration of organic matter in estuaries. *Annual Review of Marine Science* 8 (1): 409434. https://doi.org/10.1146/annurev-marine-122414-034058.

Caut, S., E. Angulo, and F. Courchamp. 2009. Variation in discrimination factors ($\Delta^{15}N$ and $\Delta^{13}C$): The effect of diet isotopic values and applications for diet reconstruction. *Journal of Applied Ecology* 46 (2): 443–453. https://doi.org/10.1111/j.1365-2664.2009.01620.x.

Cauvy-Fraunié, S., and O. Dangles. 2019. A global synthesis of biodiversity responses to glacier retreat. *Nature Ecology and Evolution* 3 (12): 1675–1685. https://doi.org/10.1038/s41559-019-1042-8.

Chester, A.J., and J.D. Larrance. 1981. Composition and vertical flux of organic matter in a large Alaskan estuary. *Estuaries* 4 (1): 42–52. https://doi.org/10.2307/1351541.

Claudino, M.C., A.L.M. Pessanha, F.G. Araújo, and A.M. Garcia. 2015. Trophic connectivity and basal food sources sustaining tropical aquatic consumers along a mangrove to ocean gradient. *Estuarine, Coastal and Shelf Science* 167: 45–55. https://doi.org/10.1016/j.ecss.2015.07.005.

Cloern, J.E., A.D. Jassby, T.S. Schraga, E. Nejad, and C. Martin. 2017. Ecosystem variability along the estuarine salinity gradient: Examples from long-term study of San Francisco Bay. *Limnology and Oceanography* 62: S272–S291. https://doi.org/10.1002/lno.10537.

Connelly, T.L., J.W. McClelland, B.C. Crump, C.T. Kellogg, and K.H. Dunton. 2015. Seasonal changes in quantity and composition of suspended particulate organic matter in lagoons of the Alaskan Beaufort Sea. *Marine Ecology Progress Series* 527: 31–45. https://doi.org/10.3354/meps11207.

Corbisier, T.N., L.S.H. Soares, M.A.V. Petti, E.Y. Muto, M.H.C. Silva, J. McClelland, and I. Valiela. 2006. Use of isotopic signatures to assess the food web in a tropical shallow marine ecosystem of Southeastern Brazil. *Aquatic Ecology* 40 (3): 381–390. https://doi.org/10.1007/s10452-006-9033-7.

de Jennings, R.M., J.J. Moran, Z.J. Jay, J.P. Beam, L.M. Whitmore, M.A. Kozubal, H.W. Kreuzer, and W.P. Inskeep. 2017. Integration of metagenomic and stable carbon isotope evidence reveals the extent and mechanisms of carbon dioxide fixation in high-temperature microbial communities. *Frontiers in Microbiology* 8: 1–11. https://doi.org/10.3389/fmicb.2017.00088.

DeNiro, M.J., and S. Epstein. 1977. Mechanism of carbon isotope fractionation associated with lipid synthesis. *Science* 197 (4300): 261–263. https://doi.org/10.1126/science.327543.

Dial, R.J., T. Scott Smeltz, P.F. Sullivan, C.L. Rinas, K. Timm, J.E. Geck, and E.C. Berg. 2016. Shrubline but not treeline advance matches climate velocity in montane ecosystems of south-central Alaska. *Global Change Biology*, 22 (5): 1841–1856. https://doi.org/10.1111/gcb.13207

Duggins, D., C.A. Simenstad, and J.A. Estes. 1989. Magnification of secondary production by kelp detritus in coastal marine ecosystems. *Science* 245 (4914): 170–173. https://doi.org/10.1126/science.245.4914.170.

Dunne, T., J.E. Richey, and B.R. Forsberg. 1998. Exchange of sediment between the floodplain and channel of the Amazon River in Brazil. *Geological Society of America Bulletin* 110 (4): 150–167. https://doi.org/10.1130/0016-7606(1998)110<0450:EOSBTF>2.3.CO;2.

Dunton, K.H., S.V. Schonberg, and L.W. Cooper. 2012. Food web structure of the Alaskan nearshore shelf and estuarine lagoons of the Beaufort Sea. *Estuaries and Coasts* 35: 416–435. https://doi.org/10.1007/s12237-012-9475-1.

Fairbanks, D., Jr., V. McArthur, C. Young, and R. Rader. 2018. Consumption of terrestrial organic matter in the rocky intertidal zone along the central Oregon coast. 9 (3). https://doi.org/10.1002/ecs2.2138.

Fellman, J.B., R.G.M. Spencer, P.J. Hernes, R.T. Edwards, D.V. D'Amore, and E. Hood. 2010. The impact of glacier runoff on the biodegradability and biochemical composition of terrigenous dissolved organic matter in near-shore marine ecosystems. *Marine Chemistry* 121 (1–4): 112–122. https://doi.org/10.1016/j.marchem.2010.03.009.

Fellman, J.B., E. Hood, P.A. Raymond, J. Hudson, M. Bozeman, and M. Arimitsu. 2015. Evidence for the assimilation of ancient glacier organic carbon in a proglacial stream food web. *Limnology and Oceanography* 60 (4): 1118–1128. https://doi.org/10.1002/lno.10088.

Fiers, G., S. Bertrand, M. Van Daele, E. Granon, B. Reid, W. Vandoorne, and M. De Batist. 2019. Hydroclimate variability of northern Chilean Patagonia during the last 20 kyr inferred from the bulk organic geochemistry of Lago Castor sediments (45°S). *Quaternary Science Reviews* 204: 105–118. https://doi.org/10.1016/j.quascirev.2018.11.015.

France, R.L. 1995. Source variability in δ15N of autotrophs as a potential aid in measuring allochthony in freshwaters. *Ecography* 18 (3): 318–320.http://www.jstor.org/stable/3682812

Fraley, K.M., M.D. Robards, M.C. Rogers, J. Vollenweider, B. Smith, A. Whiting, and T. Jones. 2021. Freshwater input and ocean connectivity affect habitats and trophic ecology of fishes in Arctic coastal lagoons. *Polar Biology*. https://doi.org/10.1007/s00300-021-02895-4.

Giordano, M., J. Beardall, and J.A. Raven. 2005. CO_2 concentrating mechanisms in algae: Mechanisms, environmental modulation, and evolution. *Annual Review of Plant Biology* 56: 99–131. https://doi.org/10.1146/annurev.arplant.56.032604.144052.

Godsey, S.E., J.W. Kirchner, and D.W. Clow. 2009. Concentration-discharge relationships reflect chemostatic characteristics of US catchments. *Hydrological Processes* 23 (13): 1844–1864. https://doi.org/10.1002/hyp.7315.

Griffiths, R.P., B.A. Caldwell, and R.Y. Morita. 1982. Seasonal changes in microbial heterotrophic activity in subarctic marine waters as related to phytoplankton primary productivity. *Marine Biology* 71: 121–127. https://doi.org/10.1007/BF00394619.

Guest, M.A., and R.M. Connolly. 2005. Fine-scale movement and assimilation of carbon in saltmarsh and mangrove habitat by resident animals. *Aquatic Ecology* 38 (4): 599–609. https://doi.org/10.1007/s10452-005-0442-9.

Guo, F., M.J. Kainz, F. Sheldon, and S.E. Bunn. 2016. The importance of high-quality algal food sources in stream food webs - current status and future perspectives. *Freshwater Biology* 61 (6): 815–831. https://doi.org/10.1111/fwb.12755.

Haglund, A.L., and H. Hillebrand. 2005. The effect of grazing and nutrient supply on periphyton associated bacteria. *FEMS Microbiology Ecology* 52 (1): 31–41. https://doi.org/10.1016/j.femsec.2004.10.003.

Harris, C.M., N.D. McTigue, J.W. McClelland, and K.H. Dunton. 2018. Do high arctic coastal food webs rely on a terrestrial carbon subsidy? *Food Webs* 15: e00081. https://doi.org/10.1016/j.fooweb.2018.e00081.

Hood, E., and D. Scott. 2008. Riverine organic matter and nutrients in southeast Alaska affected by glacial coverage. *Nature Geoscience* 1 (9): 583–587. https://doi.org/10.1038/ngeo280.

Hood, E., J. Fellman, R.G.M. Spencer, P.J. Hernes, R. Edwards, D. Damore, and D. Scott. 2009. Glaciers as a source of ancient and labile organic matter to the marine environment. *Nature* 462 (7276): 1044–1047. https://doi.org/10.1038/nature08580.

Hood, E., T.J. Battin, J. Fellman, S. O'Neel, and R.G.M. Spencer. 2015. Storage and release of organic carbon from glaciers and ice sheets. *Nature Geoscience* 8 (2): 91–96. https://doi.org/10.1038/ngeo2331.

Hope, D., M.F. Billett, and M.S. Cresser. 1994. A review of the export of carbon in river water: Fluxes and processes. *Environmental Pollution* 84 (3): 301–324. https://doi.org/10.1016/0269-7491(94)90142-2.

Hounshell, A.G., J.C. Rudolph, B.R. Van Dam, N.S. Hall, C.L. Osburn, and H.W. Paerl. 2019. Extreme weather events modulate processing and export of dissolved organic carbon in the Neuse River Estuary, NC. *Estuarine, Coastal and Shelf Science* 219: 189–200. https://doi.org/10.1016/j.ecss.2019.01.020.

Howe, E.R., and C.A. Simenstad. 2015. Using stable isotopes to discern mechanisms of connectivity in estuarine detritus-based food webs. *Marine Ecology Progress Series* 518: 13–29. https://doi.org/10.3354/meps11066.

Huss, M., and R. Hock. 2018. Global-scale hydrological response to future glacier mass loss. *Nature Climate Change* 8 (2): 135–140. https://doi.org/10.1038/s41558-017-0049-x.

IPCC. 2007. Climate change 2007: synthesis report. In *Contribution of working groups I, II and III to the fourth assessment report of the intergovernmental panel on climate change core writing team*, ed. R.K. Pachauri and A. Reisinger, 104. Switzerland IPCC: Geneva.

Jenckes, J., D.E. Ibarra, and L.A. Munk. 2022. Concentration-discharge patterns across the Gulf of Alaska reveal geomorphological and glacierization controls on stream water solute generation and export. *Geophysical Research Letters* 49 (1): 1–12. https://doi.org/10.1029/2021GL095152.

Jenckes, J., L.A. Munk, D.E. Ibarra, D.F. Boutt, J. Fellman, and E. Hood. 2023. Hydroclimate drives seasonal riverine export across a gradient of glacierized high-latitude coastal catchments. *Water Resources Research* 59: e2022WR033305. https://doi.org/10.1029/2022WR033305.

Johnson, M.A. 2021. Subtidal surface circulation in lower Cook Inlet and Kachemak Bay,Alaska. *Regional Studies in Marine Science* 41 (1). https://doi.org/10.1016/j.rsma.2021.101609.

Kamio, M., and C.D. Derby. 2017. Finding food: How marine invertebrates use chemical cues to track and select food. *Natural Product Reports* 34 (5): 514–528. https://doi.org/10.1039/c6np00121a.

Keller, K., and F.M.M. Morel. 1999. A model of carbon isotopic fractionation and active carbon uptake in phytoplankton. *Marine Ecology Progress Series* 182: 295–298. https://doi.org/10.3354/meps182295.

Konar, B., K. Iken, J.J. Cruz-Motta, L. Benedetti-Cecchi, A. Knowlton, G. Pohle, P. Miloslavich, M. Edwards, T. Trott, E. Kimani, and R. Riosmena-Rodriguez. 2010. Current patterns of macroalgal diversity and biomass in northern hemisphere rocky shores. *PLoS One1* 5 (10): e13195. https://doi.org/10.1371/journal.pone.0013195.

Kozloff, E.N. 1996. *Marine invertebrates of the Pacific Northwest*. University of Washington Press.

Kusky, T.M., and D.C. Bradley. 1999. Kinematic analysis of mélange fabrics: examples and applications from the McHugh complex, Kenai Peninsula, Alaska. *Journal of Structural Geology* 21 (12): 1773–1796. https://doi.org/10.1016/S0191-8141(99)00105-4.

Lafrenière, M.J., and M.J. Sharp. 2005. A comparison of solute fluxes and sources from glacial and non-glacial catchments over contrasting melt seasons. *Hydrological Processes* 19 (15): 2991–3012. https://doi.org/10.1002/hyp.5812.

Lammers, J.M., G.J. Reichart, and J.J. Middelburg. 2017. Seasonal variability in phytoplankton stable carbon isotope ratios and bacterial carbon sources in a shallow Dutch lake. *Limnology and Oceanography* 62 (6): 2773–2787. https://doi.org/10.1002/lno.10605.

Langdon, C., and R. Newell. 1990. Utilization of detritus and bacteria as food sources by two bivalve suspension-feeders, the oyster *Crassostrea virginica* and the mussel *Geukensia demissa Marine Ecology Progress Series* 58 (1): 299–310. https://doi.org/10.3354/meps058299.

Lee, B.J., J. Kim, J. Hur, I.H. Choi, E. Toorman, M. Fettweis, and J.W. Choi. 2019. Seasonal dynamics of organic matter composition and its effects on suspended Sediment flocculation in river water. *Water Resources Research* 55: 6968–6985. https://doi.org/10.1029/2018WR024486.

Legendre, P., and M.J. Anderson. 1999. Distance-based redundancy analysis: Testing multispecies responses in multifactorial ecological experiments. *Ecological Monographs* 69: 1–24. https://doi.org/10.1890/0012-9615(1999)069[0001:DBRATM]2.0.CO;2.

Li, X., J. Xu, Z. Shi, and R. Li. 2019. Response of bacterial metabolic activity to the river discharge in the Pearl River estuary: Implication for CO_2 degassing fluxes. *Frontiers in Microbiology* 10: 1–11. https://doi.org/10.3389/fmicb.2019.01026.

Lima-Júnior, S.E., and R. Goitein. 2001. A new method for the analysis of fish stomach contents. *Acta Scientiarum* 23: 421–424.

Lowe, A.T., A.W.E. Galloway, J.S. Yeung, M.N. Dethier, and D.O. Duggins. 2014. Broad sampling and diverse biomarkers allow characterization of nearshore particulate organic matter. *Oikos* 123 (11): 1341–1354. https://doi.org/10.1111/oik.01392.

MacIntyre, H.L., R.J. Geider, and D.C. Miller. 1996. Microphytobenthos: the ecological role of the "secret garden" of unvegetated, shallow-water marine habitats. I. Distribution, abundance and primary production. *Estuaries* 19 (2): 186–201. https://doi.org/10.2307/1352224.

McCutchan, J.H., W.M. Lewis, C. Kendall, and C.C. McGrath. 2003. Variation in trophic shift for stable isotope ratios of carbon, nitrogen, and sulfur. *Oikos* 102 (2): 378–390. https://doi.org/10.1034/j.1600-0706.2003.12098.x.

Mcmahon, K.W., W.G. Ambrose, M.J. Reynolds, and B.J. Johnson. 2021. Arctic lagoon and nearshore food webs: relative contributions of terrestrial organic matter, phytoplankton, and phytobenthos vary with consumer foraging dynamics. *Estuarine, Coastal and Shelf Science* 257: 107388. https://doi.org/10.1016/j.ecss.2021.107388.

McTigue, N.D., and K.H. Dunton. 2017. Trophodynamics of the Hanna Shoal ecosystem (Chukchi Sea, Alaska): Connecting multiple end-members to a rich food web. *Deep-Sea Research II* 144: 175–189. https://doi.org/10.1016/j.dsr2.2017.08.010.

Moore, J., and B. Semmens. 2008. Incorporating uncertainty and prior information into stable isotope mixing models. *Ecology Letters* 11: 470–480. https://doi.org/10.1111/j.1461-0248.2008.01163.x.

Muench, R.D., H.O. Mofjeld, and R.L. Charnell. 1978. Oceanographic conditions in lower Cook Inlet: Spring and summer 1973. *Journal of Geophysical Research: Oceans* 83 (C10): 5090–5098. https://doi.org/10.1029/JC083iC10p05090.

Neal, E.G., E. Hood, and K. Smikrud. 2010. Contribution of glacier runoff to freshwater discharge into the Gulf of Alaska. *Geophysical Research Letters* 37 (6): 1–5. https://doi.org/10.1029/2010GL042385.

Oksanen, J., F.G. Blanchet, M. Friendly, R. Kindt, P. Legendre, D. McGlinn, P.R. Minchin, R.B. O'Hara, G.L. Simpson, P. Solymos, M.H.H. Stevens, E. Szoecs, and H. Wagner. 2019. vegan. Community ecology package. r package version 2: 5–5.

O'Neel, S., E. Hood, A.L. Bidlack, S.W. Fleming, M.L. Arimitsu, A. Arendt, and S. Pyare. 2015. Icefield-to-ocean linkages across the Northern Pacific coastal temperate rainforest ecosystem. *BioScience* 65 (5): 499–512. https://doi.org/10.1093/biosci/biv027.

Österblom, H., O. Olsson, T. Blenckner, and R.W. Furness. 2008. Junk-food in marine ecosystems. *Oikos* 117 (7): 967–977. https://doi.org/10.1111/j.0030-1299.2008.16501.x.

Parnell, A.C., D.L. Phillips, S. Bearhop, B.X. Semmens, E.J. Ward, J.W. Moore, and R. Inger. 2013. Bayesian stable isotope mixing models. *Environmetrics* 24 (6): 387–399. https://doi.org/10.1002/env.2221.

Phillips, D.L., R. Inger, S. Bearhop, A.L. Jackson, J.W. Moore, A.C. Parnell, and E.J. Ward. 2014. Best practices for use of stable isotope mixing models in food-web studies. *Canadian Journal of Zoology* 92 (10): 823–835. https://doi.org/10.1139/cjz-2014-0127.

Post, D.M., C.A. Layman, D.A. Arrington, G. Takimoto, J. Quattrochi, and C.G. Montana. 2007. Getting to the fat of the matter: Models, methods, and assumptions for dealing with lipids in stable isotope analyses. *Oecologia* 152: 179–189. https://doi.org/10.1007/s0042-006-0630-x.

Pyke, G.H. 1984. Optimal foraging theory: A critical review. *Annual Review of Ecology and Systematics* 15 (1): 523–575. https://doi.org/10.1146/annurev.es.15.110184.002515.

Popp, B.N., E.A. Laws, R.R. Bidigare, J.E. Dore, K.L. Hanson, and S.G. Wakeham. 1998. Effect of phytoplankton cell geometry on carbon isotopic fractionation. *Geochimica Et Cosmochimica Acta* 62 (1): 69–77. https://doi.org/10.1016/S0016-7037(97)00333-5.

Radić, V., A. Bliss, A.C. Beedlow, R. Hock, E. Miles, and J.G. Cogley. 2014. Regional and global projections of twenty-first century glacier mass changes in response to climate scenarios from global climate models. *Climate Dynamics* 42 (1–2): 37–58. https://doi.org/10.1007/s00382-013-1719-7.

Ray, R., E. Michaud, R.C. Aller, V. Vantrepotte, G. Gleixner, R. Walcker, J. Devesa, M. le Goff, S. Morvan, and G. Thouzeau. 2018. The sources and distribution of carbon (DOC, POC, DIC) in a mangrove dominated estuary (French Guiana, South America). *Biogeochemistry* 138 (3): 297–321. https://doi.org/10.1007/s10533-018-0447-9.

Ren, Z., N. Martyniuk, I.A. Oleksy, A. Swain, and S. Hotaling. 2019. Ecological stoichiometry of the mountain cryosphere. *Frontiers in Ecology and Evolution* 7: 1–16. https://doi.org/10.3389/fevo.2019.00360.

Rooney, N., and K.S. McCann. 2012. Integrating food web diversity, structure, and stability. *Trends in Ecology & Evolution* 27 (1): 40–46. https://doi.org/10.1016/j.tree.2011.09.001.

Ross, J., N. Kinner, S. Saupe, J. Schloemer, and K. Ziervogel. 2022. Characterization of particle sedimentation in a subarctic estuary: a sediment trap study over two productivity seasons. *Estuaries and Coasts* (0123456789). https://doi.org/10.1007/s12237-022-01069-7.

Ruesink, J.L., A.C. Trimble, H. Berry, A.G. Sprenger, and M.N. Dethier. 2014. Environmental correlates of growth and stable isotopes in intertidal species along an estuarine fjord. *Estuaries and Coasts* 37 (1): 149–159. https://doi.org/10.1007/s12237-013-9645-9.

Sergeant, C.J., J.A. Falke, R.A. Bellmore, J.R. Bellmore, and R.L. Crumley. 2020. A classification of streamflow patterns across the coastal Gulf of Alaska. *Water Resources Research* 56 (2): e2019WR026127. https://doi.org/10.1029/2019WR026127.

Schlünz, B., and R.R. Schneider. 2000. Transport of terrestrial organic carbon to the oceans by rivers: Re-estimating flux- and burial rates. *International Journal of Earth Sciences* 88 (4): 599–606. https://doi.org/10.1007/s005310050290.

Sharkey, T.D., and J.A. Berry. 1985. Carbon isotope fractionation of algae as influenced by an inducible CO2 concentrating mechanism. In *Inorganic carbon uptake by aquatic photosynthetic organisms*, ed. W.J. Lucus and J.A. Berry, 389–401. New York: American Society of Plant Physiologists.

Siegert, D., B. Konar, M.R. Lindeberg, S. Saupe, and K. Iken. 2022. Trophic structure of key taxa in rocky intertidal communities in two contrasting high-latitude environments. *Deep Sea Research Part II: Topical Studies in Oceanography* 105050. https://doi.org/10.1016/j.dsr2.2022.105050.

Spurkland, T., and K. Iken. 2012. Seasonal growth patterns of *Saccharina latissima* (*Phaeophyceae, Ochrophyta*) in a glacially-influenced subarctic estuary. *Phycological Research* 60 (4): 261–275. https://doi.org/10.1111/j.1440-1835.2012.00657.x.

Stephenson, T.A., and A. Stephenson. 1949. The universal features of zonation between tide-marks on rocky coasts. *The Journal of Ecology* 37 (2): 289. https://doi.org/10.2307/2256610.

Sutfin, N.A., E.E. Wohl, and K.A. Dwire. 2016. Banking carbon: A review of organic carbon storage and physical factors influencing retention in floodplains and riparian ecosystems. *Earth Surface Processes and Landforms* 41 (1): 38–60. https://doi.org/10.1002/esp.3857.

Stock, B.C., A.L. Jackson, E.J. Ward, A.C. Parnell, D.L. Phillips, and B.X. Semmens. 2018. Analyzing mixing systems using a new generation of Bayesian tracer mixing models. *PeerJ* 6: e5096. https://doi.org/10.7717/peerj.5096.

Su, Y., and M. Yajima. 2021. R2jags: using R to run 'JAGS'. R package version 0.7–1. https://CRAN.R-project.org/package=R2jags.

Tiwari, T., F. Lidman, H. Laudon, W. Lidberg, and A.M. Ågren. 2017. GIS-based prediction of stream chemistry using landscape composition, wet areas, and hydrological flow pathways. *Journal of Geophysical Research: Biogeosciences* 122 (1): 65–79. https://doi.org/10.1002/2016JG003399.

Tranter, M., and J.L. Wadham. 2013. Geochemical weathering in glacial and proglacial environments. *Treatise on Geochemistry* 2 (7): 157–173. https://doi.org/10.1016/B978-0-08-095975-7.00505-2.

Varga, G.A., and E.S. Kolver. 1997. Microbial and animal limitations to fiber digestion and utilization. *The Journal of Nutrition* 127 (5): 819S-823S. https://doi.org/10.1093/jn/127.5.819S.

Volkman, J.K., and E. Tanoue. 2002. Chemical and biological studies of particulate organic matter in the ocean. *Journal of Oceanography* 58 (2): 265–279. https://doi.org/10.1023/A:1015809708632.

Ward, J.E., and S.E. Shumway. 2004. Separating the grain from the chaff: Particle selection in suspension- and deposit-feeding bivalves. *Journal of Experimental Marine Biology and Ecology* 300 (1): 83–130. https://doi.org/10.1016/j.jembe.2004.03.002.

Wells, M.L., P. Potin, J.S. Craigie, J.A. Raven, S.S. Merchant, K.E. Helliwell, A.G. Smith, M.E. Camire, and S.H. Brawley. 2017. Algae as nutritional and functional food sources: Revisiting our understanding. *Journal of Applied Phycology* 29 (2): 949–982. https://doi.org/10.1007/s10811-016-0974-5.

Wheatcroft, R.A., M.A. Goñi, J.A. Hatten, G.B. Pasternack, and J.A. Warrick. 2010. The role of effective discharge in the ocean delivery of particulate organic carbon by small, mountainous river systems. *Limnology and Oceanography* 55 (1): 161–171. https://doi.org/10.4319/lo.2010.55.1.0161.

Whitney, E.J., A.H. Beaudreau, and E.R. Howe. 2018. Using stable isotopes to assess the contribution of terrestrial and riverine organic matter to diets of nearshore marine consumers in a glacially influenced estuary. *Estuaries and Coasts* 41 (1): 193–205. https://doi.org/10.1007/s12237-017-0260-z.

Wiencke, C., and G. Fischer. 1990. Growth and stable carbon isotope composition of cold-water macroalgae in relation to light and temperature. *Marine Ecology Progress Series* 65: 283–292. https://doi.org/10.3354/meps065283.

Wiles, G.C., and P.E. Calkin. 1994. Late Holocene, high-resolution glacial chronologies and climate, Kenai Mountains, Alaska. *Geological Society of America Bulletin* 106 (2): 281–303. https://doi.org/10.1130/0016-7606(1994)106<0281:LHHRGC>2.3.CO;2.

Xu, J., X. Li, Z. Shi, R. Li, and Q. Li. 2018. Bacterial carbon cycling in the river plume in the northern south China Sea during summer. *Journal of Geophysical Research: Oceans* 123 (11): 8106–8121. https://doi.org/10.1029/2018JC014277.

Zaborska, A., W. Maria, J. Lege, E. Jankowska, A. Winogradow, and K. Deja. 2018. Sedimentary organic matter sources, benthic consumption and burial in west Spitsbergen fjords – Signs of maturing of arctic fjordic systems? *Journal of Marine Systems.* 180: 112–123. https://doi.org/10.1016/j.jmarsys.2016.11.005.